19

Bio-Nanorobotics: State of the Art and Future Challenges

Ummat A., Sharma G., and Mavroidis C.
Northeastern University

Dubey A.
Northeastern University, Rutgers University

19.1 Introduction

Nanotechnology can best be defined as a description of activities at the level of atoms and molecules that have applications in the real world. A nanometer is a billionth of a meter, that is, about 1/80,000 of the diameter of a human hair, or 10 times the diameter of a hydrogen atom. The size-related challenge is the ability to measure, manipulate, and assemble matter with features on the scale of 1 to 100 nm. In order to achieve cost-effectiveness in nanotechnology it will be necessary to automate molecular manufacturing. The engineering of molecular products needs to be carried out by robotic devices, which have been termed as *nanorobots*. A nanorobot is essentially a controllable machine at the nanometer or molecular scale that is composed of nanoscale components. The field of nanorobotics studies the design, manufacturing, programming, and control of the nanoscale robots.

This review chapter focuses on the state of the art in the emerging field of nanorobotics, its applications and discusses in brief some of the essential properties and dynamical laws which make this field more challenging and unique than its macroscale counterpart. This chapter is only reviewing nanoscale robotic devices and does not include studies related to nanoprecision tasks with macrorobotic devices that are usually included in the field of nanorobotics.

Nanorobots would constitute any passive or active structure capable of actuation, sensing, signaling, information processing, intelligence, swarm behavior at the nano scale. These functionalities could

JDP: "2123_ch019" — 2005/9/28 — 16:50 — page 1 — #1

be illustrated individually by a nanorobot or in combinations of nanorobots (swarm intelligence and cooperative behavior). Some of the abilities that are desirable for a nanorobot to function are:

1. *Swarm Intelligence* — decentralization and distributive intelligence
2. *Cooperative behavior* — emergent and evolutionary behavior
3. *Self-assembly and replication* — assemblage at nano scale and "*nanomaintenance*"
4. *Nanoinformation processing and programmability* — for programming and controlling nanorobots (autonomous nanorobots)
5. Nano to macroworld *interface architecture* — an architecture enabling instant access to the nanorobots and its control and maintenance

There are many differences between macro and nanoscale robots. These occur mainly in the basic laws that govern their dynamics. Macroscaled robots are essentially in the Newtonian mechanics domain whereas the laws governing nanorobots are in the molecular quantum mechanics domain. Furthermore, uncertainty plays a crucial role in nanorobotic systems. The fundamental barrier for dealing with uncertainty at the nano scale is imposed by the quantum and the statistical mechanics and thermal excitations. For a certain nanosystem at some particular temperature, there are positional uncertainties, which cannot be modified or further reduced [1].

The nanorobots are invisible to naked eye, which makes them hard to manipulate and work with. Techniques like scanning electron microscopy (SEM) and atomic force microscopy (AFM) are being employed to establish a visual and haptic interface to enable us to sense the molecular structure of these nanoscaled devices. Virtual reality (VR) techniques are currently being explored in nanoscience and biotechnology research as a way to enhance the operator's perception (vision and haptics) by approaching more or less a state of "full immersion" or "telepresence." The development of nanorobots or nanomachine components presents difficult fabrication and control challenges. Such devices will operate in microenvironments whose physical properties differ from those encountered by conventional parts. Since these nanoscale devices have not yet been fabricated, evaluating possible designs and control algorithms requires using theoretical estimates and virtual interfaces/environments. Such interfaces/simulations can operate at various levels of detail to trade-off physical accuracy, computational cost, number of components and the time over which the simulation follows the nanoobject behaviors. They can enable nanoscientists to extend their eyes and hands into the nanoworld and also enable new types of exploration and whole new classes of experiments in the biological and physical sciences. VR simulations can also be used to develop virtual assemblies of nano and bio-nanocomponents into mobile linkages and predict their performance.

Nanorobots with completely artificial components have not been realized yet. The active area of research in this field is focused more on molecular robots, which are thoroughly inspired by nature's way of doing things at nano scale. Mother Nature has her own set of molecular machines that have been working for centuries, and have been optimized for performance and design over the ages. As our knowledge and understanding of these numerous machines continues to increase, we now see a possibility of using the natural machines, or creating synthetic ones from scratch, using nature's components. This chapter focuses more on such molecular machines, called also *bio-nanorobots*, and explores various designs and research prevalent in this field. The main goal in the field of molecular machines is to use various biological elements — whose function at the cellular level creates motion, force or a signal — as machine components. These components perform their preprogrammed biological function in response to the specific physiochemical stimuli but in an artificial setting. In this way proteins and DNA could act as motors, mechanical joints, transmission elements, or sensors. If all these different components were assembled together in the proper proportion and orientation they would form nanodevices with multiple degrees of freedom, able to apply forces and manipulate objects in the nanoscale world. The advantage of using nature's machine components is that they are highly efficient and reliable.

Nanorobotics is a field, which calls for collaborative efforts between physicists, chemists, biologists, computer scientists, engineers, and other specialists to work towards this common objective. Figure 19.1 shows various fields, that are involved in the study of bio-nanorobotics (this is just a representative figure and not exhaustive in nature). Currently this field is still evolving, but several substantial steps have been

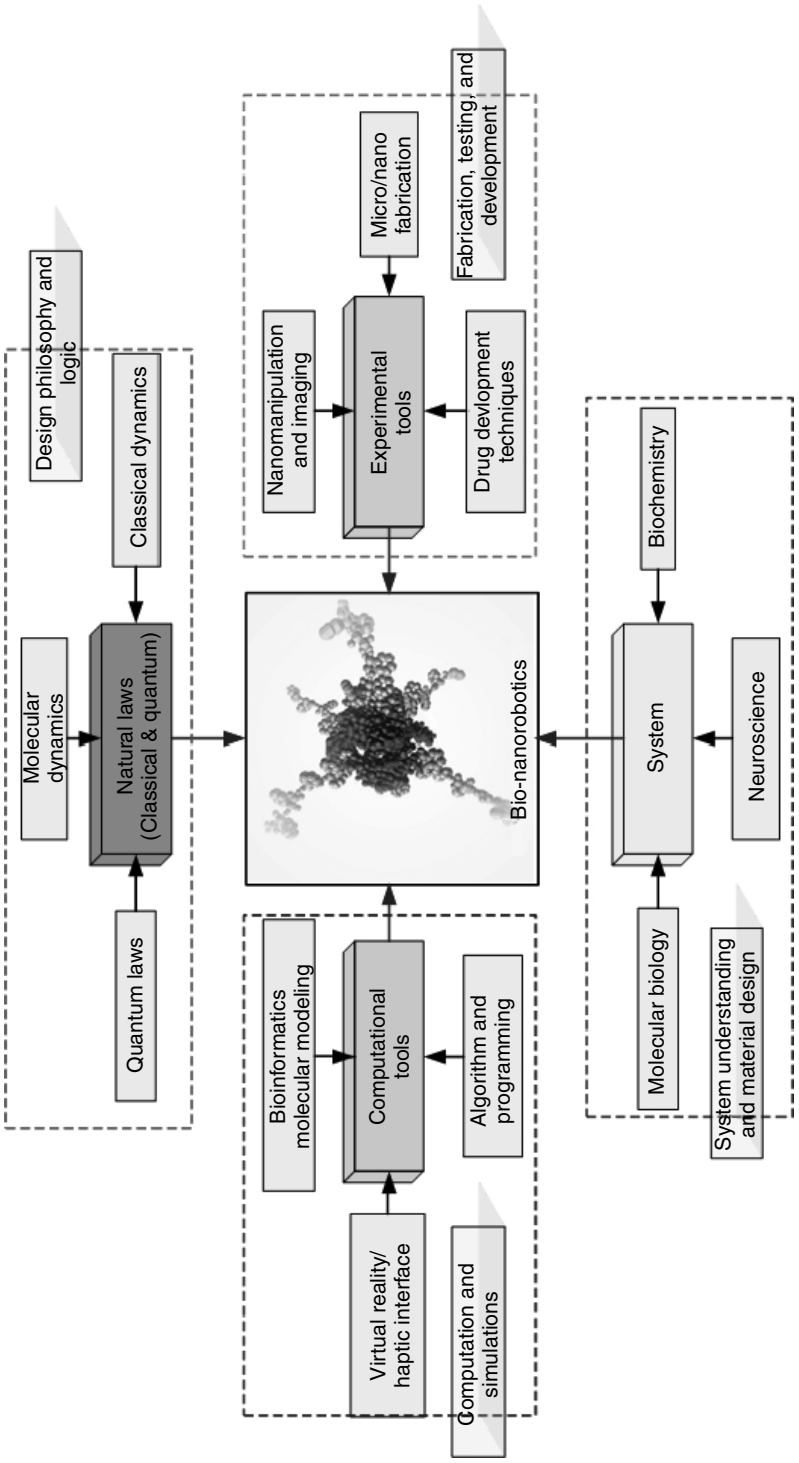

FIGURE 19.1 (See color insert following pages xxx) Bio-nanorobotics — a truly multidisciplinary field.

taken by great researchers all over the world and are contributing to this ever challenging and exciting field.

The ability to manipulate matter at the nano scale is one core application for which nanorobots could be the technological solution. A lot has been written in the literature about the significance and motivation behind constructing a nanorobot. The applications range from medical to environmental sensing to space and military applications. Molecular construction of complex devices could be possible by nanorobots of the future. From precise drug delivery to repairing cells and fighting tumor cells, nanorobots are expected to revolutionize the medical industry in the future. These applications come under the field of nanomedicine, which is a very active area of research in nanotechnology. These molecular machines hence form the basic enablers of future nanoscale applications.

In the next section, we shall try to understand the principles, theory, and utility of the known molecular machines and look into the design and control issues for their creation and modification. A majority of natural molecular machines are protein-based, while the DNA-based molecular machines are mostly synthetic. Nature deploys proteins to perform various cellular tasks — from moving cargo, to catalyzing reactions, while it has kept DNA as an information carrier. It is hence understandable that most of the natural machinery is built from proteins. With the powerful crystallographic techniques available in the modern world, the protein structures are clearer than ever. The ever-increasing computing power makes it possible to dynamically model protein folding processes and predict the conformations and structure of lesser known proteins. All this helps unravel the mysteries associated with the molecular machinery and paves the way for the production and application of these miniature machines in various fields including medicine, space exploration, electronics, and military.

19.2 Nature's Nanorobotic Devices

In this section we will detail some of the man-made and naturally occurring molecular machines. We divide the molecular machines into three broad categories — protein-based, DNA-based, and chemical molecular motors.

19.2.1 Protein-Based Molecular Machines

This section focuses on the study of the following main protein-based molecular machines:

1. ATP Synthase
2. The kinesin, myosin, dynein, and flagella molecular motors

19.2.1.1 ATP Synthase — A True Nanorotary Motor [2]

Synthesis of ATP is carried out by an enzyme, known as ATP Synthase. The inner mitochondrial membrane contains the ATP Synthase. The ATP Synthase is actually a combination of two motors functioning together as described in Figure 19.2 [3].

This enzyme consists of a proton-conducting F_0 unit and a catalytic F_1 unit. The figure also illustrates the subunits inside the two motor components. F_1 constitutes of $\alpha_3\beta_3\gamma\delta\varepsilon$ subunits. F_0 has three different protein molecules, namely, subunit a, b, and c. The γ subunit of F_1 is attached to the c subunit of F_0 and is hence rotated along with it. The $\alpha_3\beta_3$ subunits are fixed to the b subunit of F_0 and hence do not move. Further the b subunit is held inside the membrane by a subunit of F_0 (shown in Figure 19.2 by Walker [3]).

19.2.1.1.1 ATP Synthase "Nano" Properties

19.2.1.1.1.1 Reversibility of the ATP Synthase — There are two directions in ATP Synthase system and these two directions correspond to two different functionalities and behavior. This two-way behavior is because of the reversible nature of the ATP–ADP cycle and the structure of the ATP Synthase. Let us term the forward direction as when the F_0 drives the γ subunit (because of proton motive force) of F_1 and hence ATP synthesis takes place. And the backward direction is when hydrolysis of ATP counter-rotated the γ subunit and hence the F_0 motor and leads to pumping back the protons. Therefore, the forward direction

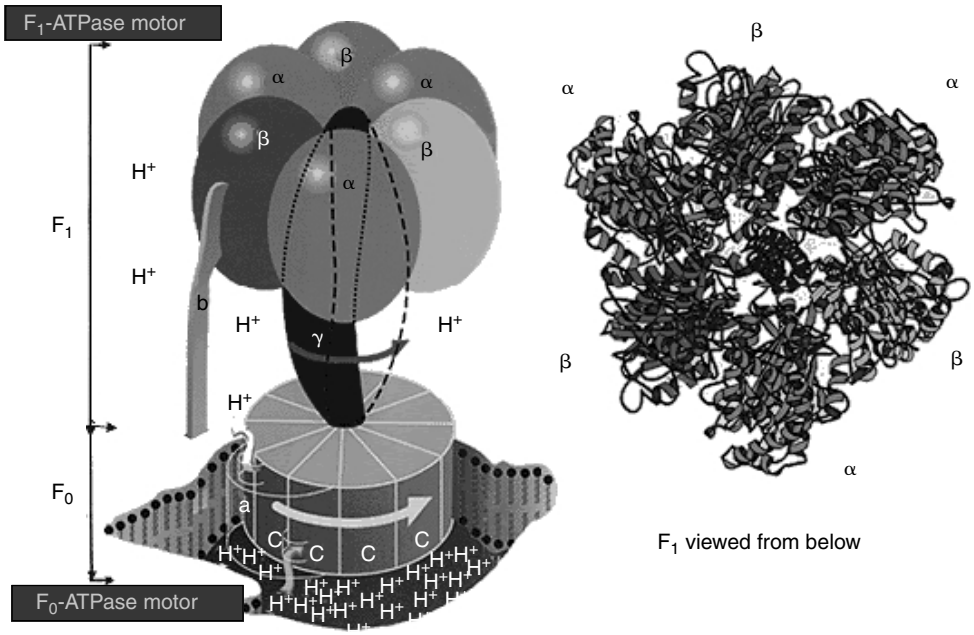

FIGURE 19.2 (See color insert) The basic structure of the ATP Synthase. Shown is the flow of protons from the outer membrane towards the inner through the F_0 motor. This proton motive force is responsible for the synthesis of ATP in F_1.

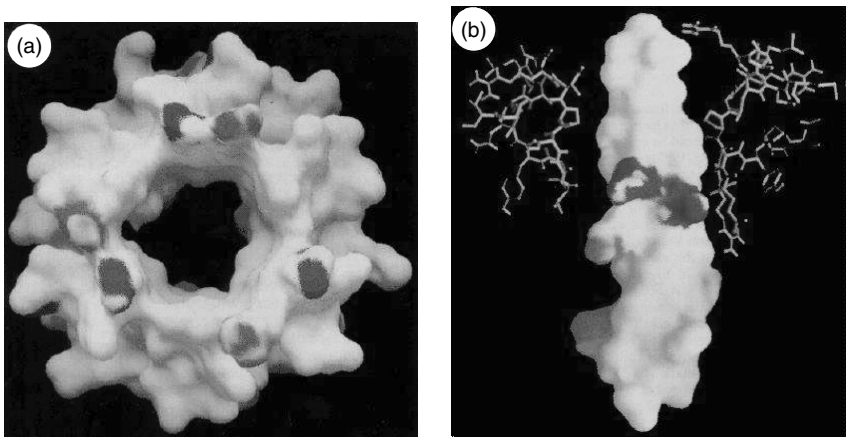

FIGURE 19.3 (See color insert) The electrostatic surface potential on the $\alpha_3\beta_3$ and γ subunits.

is powered by the proton motive force and the backward direction is powered by the ATP hydrolysis. Which particular direction is being followed depends upon the situation and the environmental factors around the ATP Synthase.

19.2.1.1.1.2 Coupling of Proton Flow (F_0) and the ATP Synthesis and Hydrolysis (in F_1) — Boyer proposed a model which predicted that the F_0 and F_1 motors are connected through the γ subunit. Further he proposed that this connection was mechanical in nature. Figure 19.3 [4] illustrates the electrostatic surface potential on $\alpha_3\beta_3$subunits. The red color represents a negatively charged surface and blue a positively charged surface. Shown in the Figure 19.3(a), a predominately neutral hole in the $\alpha_3\beta_3$subunit through which

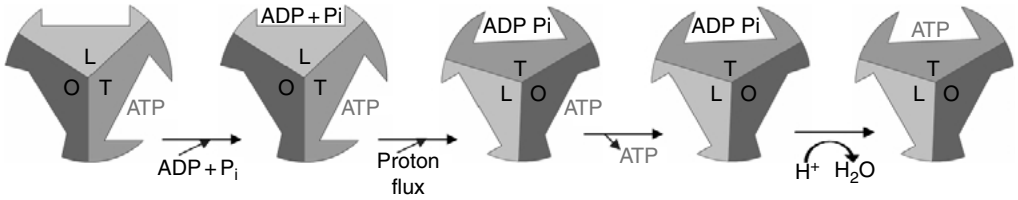

FIGURE 19.4 (See color insert) Boyer's binding change mechanism.

the γ subunit protrudes. Figure 19.3(b) shows a γ subunit with a significantly negatively charged region around half across its length. The γ subunit slides through the hole of the $\alpha_3\beta_3$ subunits.

19.2.1.1.1.3 Boyer's Binding Change Mechanism — Boyer isolated the F_1 part of the ATP Synthase complex. It was found that the α and β subunits alternate in this cylindrical part of the F_1 structure. As per this model each α and β pair forms a catalytic site. The rotation of the γ subunit induces structural conformation in the $\alpha_3\beta_3$ subunits. Although the three catalytic units are identical in their chemistry, they are functionally very different at any given point in time. These conformal changes induce a change in the binding affinities of all the three catalytic sites towards the ATPase reactants (ADP, P_i, ATP, etc.). Figure 19.4 [5] shows the binding change mechanism as proposed by Boyer.

The three catalytic sites could be in three distinct forms. O form stands for open which implies that it has got very low affinity for reactants; L form stands for loose, which implies that it would bind the reactants loosely but is still catalytically inactive; T form stands for tight, which binds the reactant tightly and is catalytically active.

The situation depicted in Figure 19.4 shows one of the sites being bound to ATP at T. The site for ADP and P_i would probably be L as it is more binding than the O site. Now when the energy is input to the system the sites are changed. T becomes O, O becomes L, and L becomes T. Due to these changes the ATP which was previously in T is now released. Further the ADP and P_i are now tightly bound due to the conversion of L site to the T site. This tight binding of ADP and P_i allows them to spontaneously get converted into ATP. Hence, this model proposed that the proton flow from the F_0 is coupled to the site inter conversions in the F_1 unit which triggers synthesis–hydrolysis of ATP. Boyer's theory was supported when Walker and his group solved the structure of the F_1-ATPase motor. The high-resolution structure thus obtained gave hints towards many experiments which proved the fact that the γ subunit indeed rotated against the α and β subunits.

19.2.1.1.1.4 F_1-ATPase a True Nanorotary Motor — Till today the exact mechanism of the molecular motor characterized by F_1-ATpase has not been fully determined. Research by Kinosita's lab is a step towards this goal and proposes some very conclusive models for the same. The results obtained show not only the various methods through which we can analyze these nanodevices, but also predicts many characteristics for these.

What is known till now is that the γ subunit rotates inside the α–β hexamer, but whether the rotation is continuous or random was not known. Kinosita's lab solved this problem by imaging the F_1-ATPase molecule. The objective of their experiment was to determine the uniqueness of the rotary motion and its characteristics. Figure 19.5 [2] depicts the experiment that was performed by this group. They attached a micrometer long actin filament to the γ subunit. This actin filament was fluorescently labeled, so that its fluorescence could be measured under a microscope. Hydrolysis of the ATP (when introduced in the experiment) led to the rotation of the γ subunit and in effect the rotation of the actin filament. As reported by the authors, not all the actin filaments were observed to have rotation. But some percentage of them did rotate and that too in a unique direction and without having much reversibility in the direction. This direct imaging proved that the structure solved by Walker and group was indeed correct and there exists rotary motion between γ subunit and the α and β hexamer.

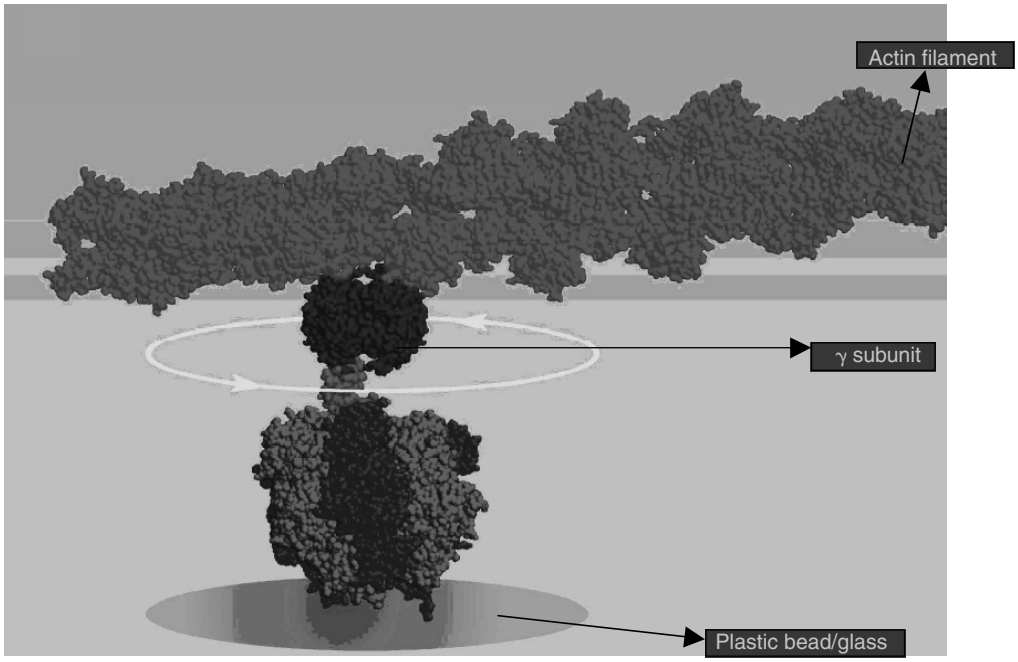

FIGURE 19.5 (See color insert) Experiment performed for Imaging of F_1-ATPase (Kinosita, K., Jr., Yasuda, R., Noji, H., and Adachi, K. 2000. *Philos. Trans.: Biol. Sci.* 355 (1396): 473–489. With permission).

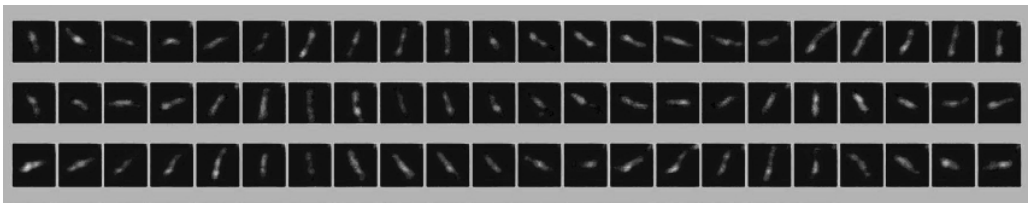

FIGURE 19.6 (See color insert) Images of a rotating actin filament (sequential image at 33 ms intervals)(Kinosita, K., Jr., Yasuda, R., Noji, H., and Adachi, K. 2000. *Philos. Trans.: Biol. Sci.* 355 (1396): 473–489. With permission).

Figure 19.6 [2] shows the imaging of the actin filament that was obtained. The rotation is not restricted to some particular rotational angle but is continuously progressive in a particular direction. As the rotational motion is a continuous one, possibility of it being a twisting motion is ruled out. Hence, there should be no direct linkage between the γ subunit and the α–β hexamer in F_1-ATPase. It was further observed by the authors that the rotation of the actin filament was in certain steps. These step sizes were approximately equal to 120°.

19.2.1.1.2 Other Observed Behaviors of the F_1-ATPase Motor [2]

19.2.1.1.2.1 Rotational Rates [2] — Rotational rates were dependent upon the length of the actin filament. Rotational rates were found to be inversely proportional to the filament length. This could be attributed to the fact that the hydrodynamic friction is proportional to the cube of the length of the filament, therefore, longer length implied that the frictional forces were higher and rotational speeds in effect slower. As reported in the principle article, if the filament were to rotate at the speed of 6 rev/sec and the length of the actin filament were 1 μm, then as per the relation:

$$N = \omega\xi$$

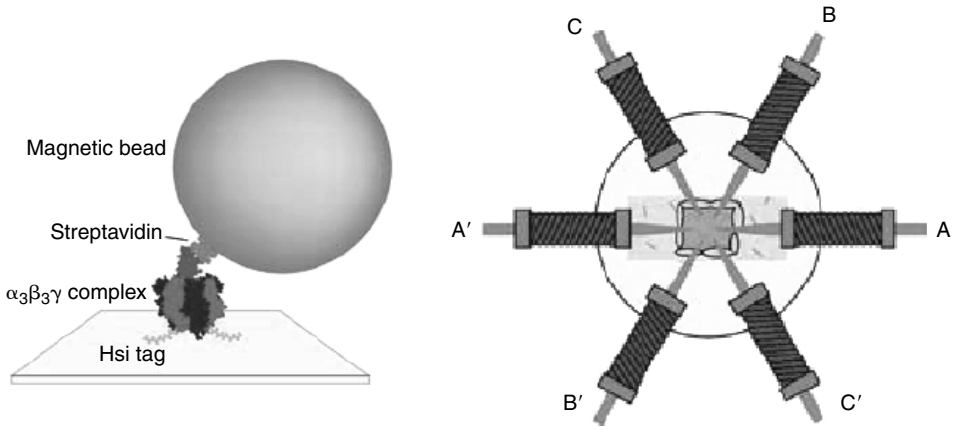

FIGURE 19.7 (See color insert) Magnetic bead is attached to the γ subunit here (left figure) and the arrangement of the magnets (right figure) [6].

The torque required would be 40 pN nm. Here ξ is the drag coefficient given by the relation:

$$\xi = \frac{4\pi}{3}\eta L^3 \frac{1}{[\ln(L/r) - 0.447]}$$

where μ is the viscosity of the medium $= 10^{-3}$ N sec/m^2 and $r = 5$ nm, the radius of the filament.

19.2.1.1.2.2 Efficiency of F_1[2] — Work done in one step, that is, 120° rotation is equal to the torque generated (i.e., 40 pN nm) times the angular displacement for that step (i.e., $2\pi/3$). This comes to about 80 pN nm. The free energy obtained by the hydrolysis of one ATP molecule is:

$$\Delta G = \Delta G_0 + k_B T \frac{\ln[\text{ADP}][\text{P}_\text{i}]}{[\text{ATP}]}$$

Here, the standard free energy change per ATP molecule is equal to −50 pN nm at pH 7. The thermal energy at room temperature is equal to 4.1 pN nm. At intracellular conditions, [ATP] and [P_i] is in the order of 10^{-3} M. Therefore, for [ADP] of 50 μM, ΔG is equal to −90.604 pN nm. Comparing this value of the free energy obtained by the hydrolysis of one molecule of ATP with the mechanical work done by the motor (i.e., 80 pN nm), we can deduce that the F_1-ATPase motor works on efficiency close to 100%!

19.2.1.1.2.3 Chemical Synthesis of ATP Powered by Mechanical Energy — In another study [6], evidence has been provided to justify the claim that the chemical synthesis of ATP occurs when propelled by mechanical energy. This basic nature of the F_1-ATPase was known for quite some time, but it is the first time that it is being experimentally verified. To prove this concept, the F_1 was bound to the glass surface through histidine residues attached at the end of the γ subunits. A magnetic bead coated with streptavidin was attached to the γ subunit (Figure 19.7 [6]).

Electric magnets were used to rotate this bead attached to the γ subunit. The rotation resulted in appearance of ATP in the medium (which was initially immersed in ADP). Thus, the connection between the syntheses of ATP as a result of the mechanical energy input is established.

The exact mechanism of the F_1-ATPase rotation is still an active area of research today and many groups are working towards finding it. The key to solving the mechanism is solving the *transient conformation* of the catalytic sites and the γ subunit when rotation is taking place. What is not clear is the correspondence between the chemical reactions at the catalytic sites and their influence on the rotation of the γ subunit. Which event triggers the rotation and which does not has still to be exactly determined? Many models have been predicted, but they all still elude the reality of the rotational mechanism.

19.2.1.2 The Kinesin, Myosin, Dynein, and Flagella molecular motors

With modern microscopic tools, we view a cell as a set of many different moving components powered by molecular machines rather than a static environment. Molecular motors that move unidirectionally along protein polymers (actin or microtubules) drive the motions of muscles as well as much smaller intracellular cargoes. In addition to the F_0–F_1-ATPase motors inside the cell, there are linear transport motors present as tiny vehicles known as motor proteins that transport molecular cargoes [7] that also require ATP for functioning. These minute cellular machines exist in three families — the kinesins, the myosins, and the dyneins [8]. The cargoes can be organelles, lipids, or proteins etc. They play an important role in cell division and motility. There are over 250 kinesin-like proteins, and they are involved in processes as diverse as the movement of chromosomes and the dynamics of cell membranes. The only part they have in common is the catalytic portion known as the motor domain. They have significant differences in their location within cells, their structural organization, and the movement they generate [9]. Muscle myosin, whose study dates back to 1864, has served as a model system for understanding motility for decades. Kinesin, however, was discovered rather recently using *in vitro* motility assays in 1985 [10]. Conventional kinesin is a highly processive motor that can take several hundred steps on a microtubule without detaching [11,12] whereas muscle myosin executes a single "stroke" and then dissociates [13]. A detailed analysis and modeling of these motors has been done [10,14].

Kinesin and myosin make up for an interesting comparison. Kinesin is microtubule-based; it binds to and carries cargoes along microtubules whereas myosin is actin-based. The motor domain of kinesin weighs one third the size of that of myosin and one tenth of that of dynein [15]. Before the advent of modern microscopic and analytic techniques, it was believed that these two have little in common. However, the crystal structures available today indicate that they probably originated from a common ancestor [16].

19.2.1.2.1 The Myosin Linear Motor

Myosin is a diverse superfamily of motor proteins [17]. Myosin-based molecular machines transport cargoes along actin filaments — the two stranded helical polymers of the protein actin, about 5 to 9 nm in diameter. They do this by hydrolyzing ATP and utilizing the energy released [18]. In addition to transport, they are also involved in the process of force generation during muscle contraction, wherein thin actin filaments and thick myosin filaments slide past each other. Not all members of the myosin superfamily have been characterized as of now. However, much is known about the structure and function. Myosin molecules were first sighted through electron microscope protruding out from thick filaments and interacting with the thin actin filaments in late 1950s [19–21]. Since then it was known that ATP plays a role in myosin related muscle movement along actin [22]. However, the exact mechanism was unknown, which was explained later in 1971 by Lymn and Taylor [23].

19.2.1.2.1.1 Structure of Myosin Molecular Motor — A myosin molecule binding to an actin polymer is shown in Figure 19.8(a) [24]. Myosin molecule has a size of about 520 kD including two 220 kD heavy chains and light chains of sizes between 15 and 22 kD [25,26]. They can be visualized as two identical globular "motor heads," also known as motor domains, each comprising of a catalytic domain (actin, nucleotide as well as light chain binding sites) and about 8 nm long lever arms. The heads, also sometimes referred to as S1 regions (subfragment 1) are shown in blue, while the lever arms or the light chains, in yellow. Both these heads are connected via a coiled coil made of two α-helical coils (gray) to the thick base filament. The light chains have considerable sequence similarity with the protein "calmodulin" and troponin C, and are sometimes referred to as calmodulin-like chains. They act as links to the motor domains and do not play any role in their ATP binding activity [27] but for some exceptions [28,29]. The motor domain in itself is sufficient for moving actin filaments [30]. Three-dimensional (3D) structures of myosin head revealed that it is a pear-shaped domain, about 19 nm long and 5 nm in maximum diameter [30,31].

19.2.1.2.1.2 Function of Myosin Molecular Motor — A crossbridge-cycle model for the action of myosin on actin has been widely accepted since 1957 [19,32,33]. Since the atomic structures of actin monomer

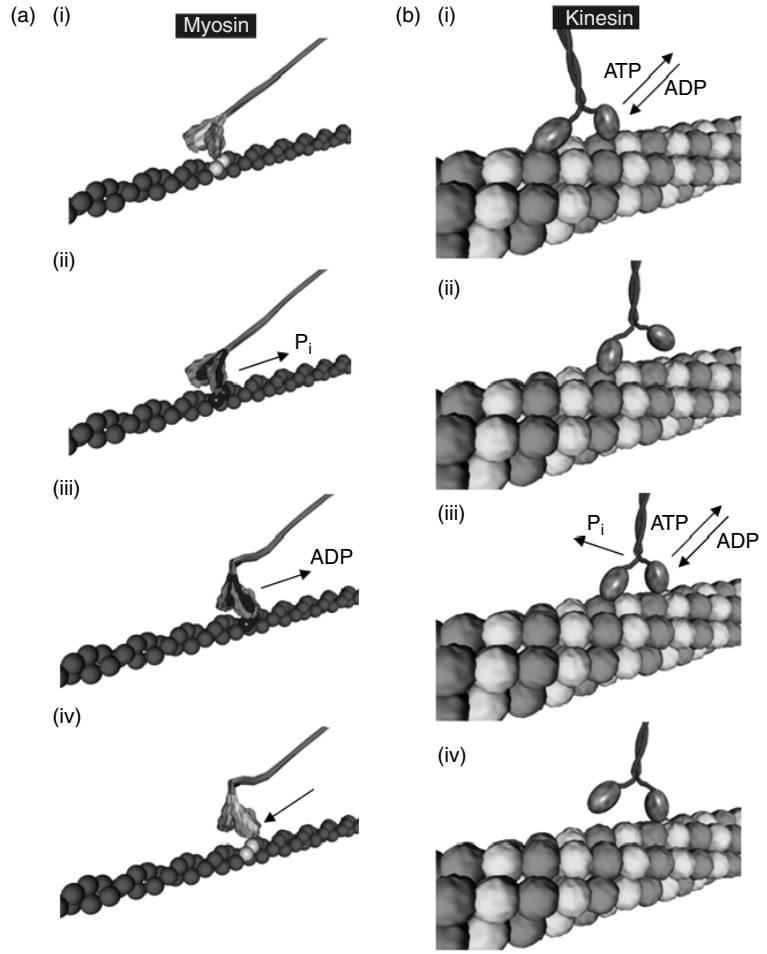

FIGURE 19.8 (See color insert) The kinesin–myosin walks: (a) Myosin motor mechanism. (i) Motor head loosely docking to the actin binding site; (ii) The binding becomes tighter along with the release of P_i; (iii) Lever arm swings to the left with the release of ADP, and; (iv) replacement of the lost ADP with a fresh ATP molecule results in dissociation of the head; (b) Kinesin heads working in conjunction. (i) Both ADP-carrying heads come near the microtubule and one of them (black neck) binds; (ii) Loss of bound ADP and addition of fresh ATP in the bound head moves the other (red neck) to the right; (iii) The second head (red) binds to microtubule while losing its ADP, and replacing it with a new ATP molecule while the first head hydrolyses its ATP and loses P_i; (iv) The ADP-carrying black-neck will now be snapped forward, and the cycle will be repeated.

[34,35] and myosin [31] were resolved, this model has been refined into a "lever-arm model," which is now acceptable [36]. Only one motor head is able to connect to the actin filament at a time, the other head remains passive. Initially, the catalytic domain in the head has ADP and P_i bound to it and as a result, its binding with actin is weak. With the active motor head docking properly to the actin-binding site, the P_i has to be released. As soon as this happens, the lever arm swings counterclockwise [37] due to a conformational change [21,38–43]. This pushes the actin filament down by about 10 nm along its longitudinal axis [44]. The active motor head now releases its bound ADP and another ATP molecule by way of Brownian motion quickly replaces it, making the binding of the head to the actin filament weak again. The myosin motor then dissociates from the actin filament, and a new cycle starts. However, nanomanipulation of single S1 molecules (motor domains) show that myosin can take multiple steps per ATP molecule hydrolyzed, moving in 5.3 nm steps and resulting in displacements of 11 to 30 nm [45].

19.2.1.2.2 The Kinesin Linear Motor

Kinesin [15] and dynein family of proteins are involved in cellular cargo transport along microtubules as opposed to actin in the case of myosin [46]. Microtubules are 25 nm diameter tubes made of protein tubulin and are present in the cells in an organized manner. Microtubules have polarity; one end being the plus (fast growing) end while the other end is the minus (slow growing) end [47]. Kinesins move from minus end to plus end, while dyneins move from plus end to the minus end of the microtubules. Microtubule arrangement varies in different cell systems. In nerve axons, they are arranged longitudinally in such a manner that their plus ends point away from the cell body and into the axon. In epithelial cells, their plus end points towards the basement membrane. They deviate radially out of the cell center in fibroblasts and macrophages with the plus end protruding outwards [48]. Like myosin, kinesin is also an ATP-driven motor. One unique characteristic of kinesin family of proteins is their processivity — they bind to microtubules and literally "walk" on it for many enzymatic cycles before detaching [49,50]. Also, each of the globular heads/motor domains of kinesin is made of one single polypeptide unlike myosin (heavy and light chains and dynein heavy, intermediate, and light chains).

19.2.1.2.2.1 Structure of Kinesin Molecular Motor — A lot of structural information about kinesin is now available through the crystal structures [16,51,52]. The motor domain contains a folding motif similar to that of myosin and G proteins [8]. The two heads or the motor domains of kinesin are linked via "neck linkers" to a long coiled coil, which extends up to the cargo (Figure 19.8[b]). They interact with the α and β subunits of the tubulin hetrodimer along the microtubule protofilament. The heads have the nucleotide and the microtubule binding domains in them.

19.2.1.2.2.2 Function of Kinesin Molecular Motor — While Kinesin is also a two-headed linear motor, its modus operandi is different from myosin in the sense that *both* its head work together in a coordinated manner rather than one was being left out. Figure 19.8(b) shows the kinesin walk. Each of the motor heads is near the microtubule in the initial state with each motor head carrying an ADP molecule. When one of the heads loosely binds to the microtubule, it looses its ADP molecule to facilitate a stronger binding. Another ATP molecule replaces the ADP, which facilitates a conformational change such that the neck region of the bound head snaps forward and zips on to the head [9]. In the process it pulls the other ADP carrying motor head forward by about 16 nm so that it can bind to the next microtubule-binding site. This results in the net movement of the cargo by about 8 nm [53]. The second head now binds to the microtubule by losing its ADP, which is promptly replaced by another ATP molecule due to Brownian motion. The first head meanwhile hydrolyses the ATP and loses the resulting P_i. It is then snapped forward by the second head while it carries its ADP forward. Hence, coordinated hydrolysis of ATP in the two motor heads is the key to the kinesin processivity [54,55]. Kinesin is able to take about 100 steps before detaching from the microtubule [11,49,56] while moving at 1000 nm/sec and exerting forces of the order of 5 to 6 pN at stall [57,58].

19.2.1.2.3 The Dynein Motor

The Dynein superfamily of proteins was introduced in 1965 [59]. Dyneins exist in two isoforms, the cytoplasmic and the axonemal. Cytoplasmic dyneins are involved in cargo movement, while axonemal dyneins are involved in producing bending motions of cilia and flagella [60–70]. Figure 19.9 shows a typical cytoplasmic dynein molecule.

19.2.1.2.3.1 Structure of Dynein Molecular Motor — The structure consists of two heavy chains in the form of globular heads, three intermediate chains and four light intermediate chains [71,72]. Recent studies have exposed a linker domain connecting the "stem" region below the heads to the head itself [73]. Also from the top of the heads the microtubule binding domains (the stalk region, not visible in the figure) protrude out [74]. The ends of these stalks have smaller ATP sensitive globular domains, which bind to the microtubules. Cytoplasmic dynein is associated with a protein complex known as dynactin, which contains ten subunits [75]. Some of them are shown in the figure as p150, p135, actin-related protein 1 (Arp1), actin, dynamitin, capping protein, and p62 subunit. These play an important regulatory role in the

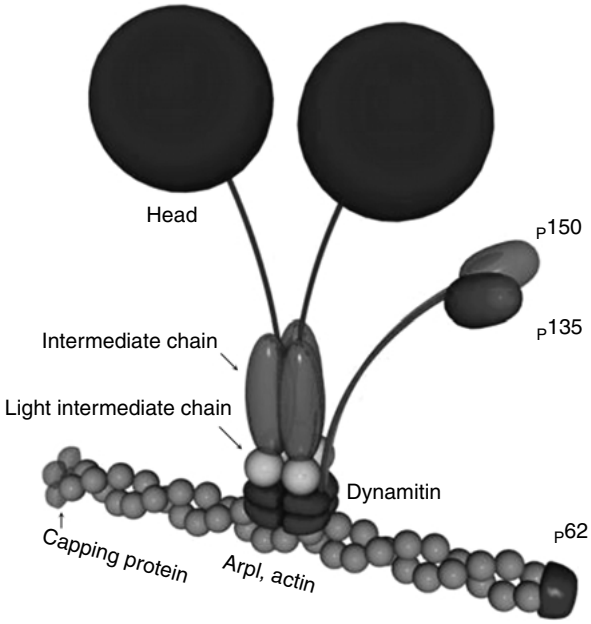

FIGURE 19.9 (See color insert) A dynein molecule. Shown in blue are the globular heads (heavy chains) connected to the intermediate chains (red) and the light chains (light blue). Dynactin complex components p150, p135, dynamitin, p62, capping proteins, Arp1, actin is also shown.

binding ability of dynein to the microtubules. The heavy chains forming the two globular heads contain the ATPase and microtubule motor domains [76].

One striking difference that dynein exhibits compared to kinesins and myosins is that dynein has AAA (ATPases Associated with a variety of cellular Activities) modules [77–79], which indicate that its mode of working will be entirely different from kinesins and myosins. This puts dyneins into the AAA superfamily of mechanoenzymes. The dynein heavy chains contain six tandemly linked AAA modules [80,81] with the head having a ring-like domain organization, typical of AAA superfamily. Four of these are nucleotide binding motifs, named P1–P4, but only P1 (AAA1) is able to hydrolyze ATP.

19.2.1.2.3.2 Function of Dynein Molecular Motor — Because dynein is larger and more complex structure as compared to other motor proteins, its mode of operation is not as well known. However, very recently, Burgess et al. [73] have used electron microscopy and image processing to show the structure of a flagellar dynein at the start and end of its power stroke, giving some insight into its possible mode of force generation. When the dynein contains bound ADP and V_i (vandate), it is in the prepower stroke conformation. The state when it has lost the two, known as the apostate is the more compact postpower stroke state. There is a distinct conformational change involving the stem, linker, head, and the stalk that produces about 15 nm of translation onto the microtubule bound to the stalk [73].

19.2.1.2.4 The Flagella Motors

Unicellular organisms, such as, *Escherichia coli* have an interesting mode of motility (for reviews see [82–84]). They have a number of molecular motors, about 45 nm in diameter, that drive their "feet" or the flagella that help the cell to swim. Motility is critical for cells, as they often have to travel from a less favorable to a more favorable environment. The flagella are helical filaments that extend out of the cell into the medium and perform a function analogous to what the oars perform to a boat. The flagella and the motor assembly are called a flagellum. The flagella motors impart a rotary motion into the flagella [85,86]. In addition to a rotary mechanism, the flagella machines consist of components such as rate meters, particle counters, and gearboxes [87]. These are necessary to help the cell decide

which way to go, depending on the change of concentration of nutrients in the surroundings. The rotary motion imparted to the flagella needs to be modulated to ensure the cell is moving in the proper direction as well as all flagella of the given cell are providing a concerted effort towards it [88]. When the motors rotate the flagella in a counterclockwise direction as viewed along the flagella filament from outside, the helical flagella create a wave away from the cell body. Adjacent flagella subsequently intertwine in a propulsive corkscrew manner and propel the bacteria. When the motors rotate clockwise, the flagella fly apart, causing the bacteria to tumble, or change its direction [89]. These reversals occur randomly, giving the bacterium a "random walk," unless of course, there is a preferential direction of motility due to reasons mentioned earlier. The flagella motors allow the bacteria to move at speeds of as much as 25 μm/sec with directional reversals occurring approximately 1 per sec [90]. A number of bacterial species in addition to *E. coli*, depend on flagella motors for motility. Some of these are *Salmonella enterica serovar Typhimurium* (Salmonella), *Streptococcus*, *Vibrio* spp., *Caulobacter*, *Leptospira*, *Aquaspirrilum serpens*, and *Bacillus*. The rotation of flagella motors is stimulated by a flow of ions through them which is a result of a build-up of a transmembrane ion gradient. There is no direct ATP-involvement, however, the proton gradient needed for the functioning of flagella motors can be produced by ATPase.

19.2.1.2.4.1 Structure of the Flagella Motors — A complete part list of the flagella motors may not be available as of now. Continued efforts dating back to early 1970s have, however, revealed much of their structure, composition, genetics, and function. Newer models of the motor function are still being proposed with an aim to explain observed experimental phenomena [91,92]. That means that we do not fully understand the functioning of this motor [83]. A typical flagella motor from *E. coli* consists of about 20 different proteins [83], while there are yet more that are involved in the assembly and functioning. There are 14 Flg-type proteins named FlgA to FlgN; 5 Flh-type proteins called FlhA to FlhE; 19 Fli-type proteins named FliA to FliT; MotA and MotB making a total of 40 related proteins. The name groups Flg, Flh, Fli, and Flg originate from the names of the corresponding genes [93]. Out of these the main structural proteins are FliC or the filament; FliD (filament cap); FliF or the MS-ring; FliG; FliM, and FliN (C-ring); FlgB, FlgC, and FlgF (proximal rod); FlgG (distal rod); FlgH (L-ring); FlgI (P-ring); FlgK and FlgL (hook-filament junction); and MotA-MotB (torque generating units). Earlier it was believed that the M and S are two separate rings and M was named after membrane and S after supramembranous [94]. Now they are jointly called the MS-ring as it has been found that they are two domains of the same protein FliF [95,96]. The C-ring is named after cytoplasmic [97–99], while the names of the P and L-rings come from "peptidoglycan" and "lipopolysaccharide," respectively. The FlhA, B, FliH, I, O, P, Q, R constitute the "transport apparatus."

The hook and filament part of the flagellum is located outside the cell body, while the motor portion is embedded in the cell membrane with parts (the C-ring and the transport apparatus) that are inside the inner membrane in the cytoplasmic region. MotA and MotB are arranged in a circular array embedded in the inner membrane, with the MS-ring at the center. Connected to the MS-ring is the proximal end of a shaft, to which the P-ring, which is embedded in the peptidoglycan layer, is attached. Moving further outwards, there is the L-ring embedded in the outer cell membrane followed by the distal shaft end that protrudes out of the cell. To this end there is an attachment of the hook and the filament, both of which are polymers of hook-protein and flagellin, respectively.

19.2.1.2.4.2 Function of the Flagella Motors — The flagellar motors in most cases are powered by protons flowing through the cell membrane (protonmotive force, defined earlier) barring exceptions such as certain marine bacteria, for example, the *Vibrio* spp., which are driven by Na^+ ions [100]. There are about 1200 protons required to rotate the motor by one rotation [101]. A complete explanation of how this proton flow is able to generate torque is not available as of today. From what is known, the stator units of MotA and MotB play an important role in torque generation. They form a MotA/MotB complex which when oriented properly binds to the peptidoglycan and opens proton channels through which protons can flow [102]. It is believed that there are eight such channels per motor [103]. The protonmotive force is a result of the difference of pH in the outside and the inside of the cell. The *E. coli* cells like to maintain

a pH of 7.6–7.8 on their inside, hence depending on the pH of the surroundings, the protonmotive force will vary, and hence the speed of rotation of their motors. To test how the speed of rotation depends on the protonmotive force, the motors were powered by external voltage with markers acting as heavy loads attached to them [104]. It was found that the rotation indeed depends directly on the protonmotive force. According to the most widely accepted model, MotA/MotB complex interacts with the rotor via binding sites. The passage of protons through a MotA/MotB complex (stator or torque generator) moves it so that they bind to the next available binding site on the rotor, thereby stretching their linkage. When the linkage recoils, the rotor assembly has to rotate by one step. Hence, whichever complex receives protons from the flux will rotate the rotor, generating torque. The torque–speed dependence of the motor has been studied in detail [105,106] and indicates the torque range of about 2700 to 4600 pN nm.

19.2.2 DNA-Based Molecular Machines

As mentioned earlier, nature chose DNA mainly as an information carrier. There was no mechanical work assigned to it. Energy conversion, trafficking, sensing, etc., were the tasks assigned mainly to proteins. Probably for this reason, DNA turns out to be a simpler structure — with only four kinds of nucleotide bases adenosine, thiamine, guanine, and cytosine (A, T, G, and C) attached in a linear fashion that take a double helical conformation when paired with a complementary strand. Such structural simplicity vis-à-vis proteins — made of 20 odd amino acids with complex folding patterns — results in a simpler structure and predictable behavior. There are certain qualities that make DNA an attractive choice for the construction of artificial nanomachines. In recent years, DNA has found use in not only mechanochemical, but also in nanoelectronic systems as well [107–110]. A DNA double-helical molecule is about 2 nm in diameter and has 3.4–3.6 nm helical pitch no matter what its base composition is; a structural uniformity is not achievable with protein structures if one changes their sequence. Furthermore, double-stranded DNA (*ds*-DNA) has a respectable persistence length of about 50 nm [111] which provides it enough rigidity to be a candidate component of molecular machinery. Single stranded DNA (*ss*-DNA) is very flexible and cannot be used where rigidity is required, however, this flexibility allows its application in machine components like hinges or nanoactuators [112]. Its persistence length is about 1 nm nm covering up to three base pairs [113] at 1 *M* salt concentration.

Other than the above structural features there are two important and exclusive properties that make DNA suitable for molecular level constructions. These are — molecular recognition and self-assembly. The nucleotide bases A and T on two different *ss*-DNA have affinity towards each other, so do G and C. Effective and stable *ds*-DNA structures are only formed if the base orders of the individual strands are complementary. Hence, if two complementary single strands of DNA are in a solution, they will eventually recognize each other and hybridize or zip-up forming a *ds*-DNA. This property of molecular recognition and self-assembly has been exploited in a number of ways to build complex molecular structures [114–121]. In the mechanical perspective, if the free energy released by hybridization of two complementary DNA strands is used to lift a hypothetical load, a force capacity of 15 pN can be achieved [122], comparable to that of other molecular machines like kinesin (5 pN) [123].

Dr. Nadrian Seeman and colleagues built the first artificial DNA-based structure in the form of a cube in 1991 [116,124]. They then went on to create more complex structures such as knots [125,126] and Borromean rings [127]. In addition to these individual constructs, 2D arrays [118,127,128] with the help of the double-crossover (DX) DNA molecule [129–131]. This DX molecule gave the structural rigidity required to create a dynamic molecular device, the B–Z switch [132]. DNA double helices can be of three types — the A, B, or the Z-DNA. The B-DNA is the natural, right-handed helical form of DNA, while the A-DNA is a shrunken, low-humidity form of the B-DNA. Z-DNA can be obtained from certain C–G base repeat sequences occurring in B-DNA that can take a left-handed double helical form [133]. The CG repeated base pair regions can be switched between the left and the right-handed conformations by changing ionic concentration [134]. The switch was designed in such a way that it had three cyclic strands of DNA, two of them wrapped around a central strand that had the CG-repeat region in the middle. On the two free ends of the side strands fluorescent dyes were attached in order to monitor the

conformational change. With the change in ionic concentration the central CG-repeat sequence could alternate between the B and the Z modes bidirectionally which was observed through Förster resonance energy transfer (FRET) spectroscopy.

19.2.2.1 The DNA Tweezers

In 2000, Dr. Bernard Yurke and colleagues made an artificial DNA based molecular machine that also accepted DNA as a fuel [135]. The machine, called DNA tweezers, consisted of three strands of DNA labeled A, B, and C. Strands B and C are partially hybridized on to the central strand A with overhangs on both ends. This conformation of the machine is the open conformation. When an auxiliary fuel strand F is introduced, that is designed to hybridize with both overhang regions, the machine attains a closed conformation. The fuel strand is then removed from the system by the introduction of its exact complement, leaving the system to go back to its original open conformation. This way, a reversible motion is produced, which can be observed by attaching fluorescent tags to the two ends of the strand A. In this case the 5′ end was labeled with the dye TET (tetrachloro-fluorescein phosphoramidite) and the 3′ end was labeled with TAMRA (carboxy-tertamethylrhodamine). Aside from the creation of a completely new molecular machine, this showed a way of selective fueling of such machines. The fuel strands are sequence-specific, hence they will work on only those machines towards which they are directed, and not trigger other machines surrounding them. This machine was later improved to form a Three-State Device [136] which had two robust states and one flexible intermediate state. A variation of the tweezers came about as the DNA-scissors [137].

19.2.3 Inorganic (Chemical) Molecular Machines

In the past two decades, chemists have been able to create, modify, and control many different types of molecular machines. Many of these machines carry a striking resemblance with our everyday macroscale machines such as gears, propellers, shuttles, etc. Not only this, all of these machines are easy to synthesize artificially and are generally more robust than the natural molecular machines. Most of these machines are organic compounds of carbon, nitrogen, and hydrogen, with the presence of a metal ion being required occasionally. Electrostatic interactions, covalent and hydrogen bonding play essential role in the performance of these machines. Such artificial chemical machines are controllable in various ways — chemically, electrochemically, and photochemically (through irradiation by light). Some of them are even controllable by more than one way, rendering more flexibility and enhancing their utility. A scientist can have more freedom with respect to the design of chemical molecular machines depending on the performance requirements and conditions. Rotaxanes [138–140] and catenanes [141,142] make the basis of many of the molecular machines described in this section. These are families of interlocked organic molecular compounds with a distinctive shape and properties that guide their performance and control.

19.2.3.1 The Rotaxanes

The Rotaxane family of molecular machines is characterized by two parts — a dumbbell shaped compound with two heavy chemical groups at the ends and a light, cyclic component, called macrocycle, interlocked between the heads as shown in Figure 19.10. It has been shown [143] that a reversible switch can be made with a rotaxane setup. For this, one needs to have two chemically active recognition sites in the neck region of the dumbbell. In this particular example, the thread was made of polyether, marked by recognition sites hydroquinol units and terminated at the ends by large triisoproplylsilyl groups. A tetracationic bead was designed and self-assembled into the system that interacts with the recognition sites.

The macrocycle has a natural low energy state on the first recognition site, but can be switched among the two sites reversibly upon application of suitable stimuli. Depending on the type of rotaxane setup the stimuli can be chemical, electrochemical, or photochemical [144,145]. The stereo-electronic properties of the recognition sites can be altered by protonation or deprotonation, or by oxidation or reduction, thereby changing their affinity towards the macrocycle. In a recent example, light-induced acceleration of

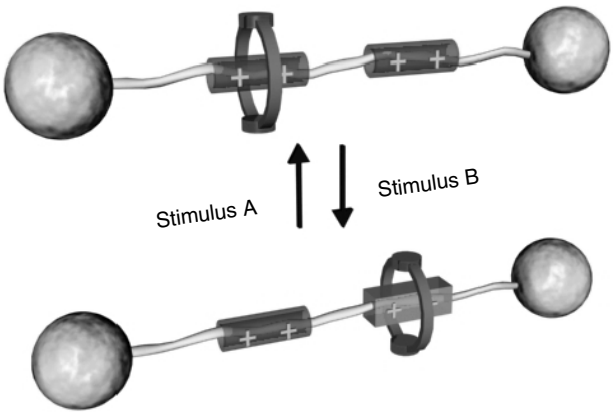

FIGURE 19.10 (See color insert) A typical rotaxane shuttle set-up. The macrocycle encircles the thread-like portion of the dumbbell with heavy groups at its ends. The thread has two recognition sites which can be altered reversibly so as to make the macrocycle shuttle between the two sites (state 0 and state 1).

rotaxane motion was achieved by photoisomerization [146], while similar controls through alternating current (oscillating electric fields) was shown before [147].

19.2.3.2 The Catenanes

The catenanes are also special type of interlocked structures that represent a growing family of molecular machines. They are synthesized by supramolecular assistance to molecular synthesis [148,149]. The general structure of a catenane is that of two interlocked ring-like components that are noncovalently linked via a mechanical bond, that is, they are held together without any valence forces. Both the macrocyclic components have recognition sites that are atoms of groups that are redox-active or photochemically reactive. It is possible to have both rings with similar recognition sites. In such a scenario, one of the rings may rotate inside the other with the conformations stabilized by noncovalent interactions, but the two states of the inner ring differing by 180° will be undistinguishable (degenerate) [150]. For better control and distinguishable molecular conformations, it is desirable to have different recognition sites within the macrocycles. Then they can be controlled independently through their own specific stimuli. The stereo-electronic property of one recognition site within a macrocycle can be varied such that at one point it has more affinity to the sites on the other ring. At this instant, the force balance will guide the rotating macrocycle for a stable conformation that requires that particular site to be inside the other macrocycle. Similarly, with other stimulus, this affinity can be turned off, or even reversed along with the affinity of the second recognition site on the rotating macrocycle increased towards those on the static one. There is a need for computational modeling, simulation, and analysis of such molecular machine motion [151]. Like rotaxanes, catenanes also can be designed for chemical, photochemical, or electrochemical control [152–156]. Figure 19.11 describes one such catenane molecular motor.

For both rotaxane and catenane-based molecular machines, it is desirable to have recognition sites such that they can be easily controlled externally. Hence, it is preferable to build sites that are either redox-active or photo-active [144]. Catenanes can also be self-assembled [157]. An example of catenane assembled molecular motors is the electronically controllable bistable switch [158]. An intuitive way of looking at catenanes is to think of them as molecular equivalents of ball and socket and universal joints [153,159,160].

Pseudorotaxanes are structures that contain a ring-like element and a thread-like element that can be "threaded" or "dethreaded" onto the ring upon application of various stimuli. Again, the stimuli can be chemical, photochemical, or electrochemical [161]. These contain a promise of forming molecular machine components analogous to switches and nuts and bolts from the macroscopic world.

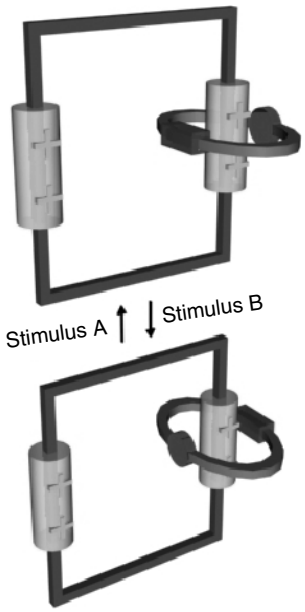

FIGURE 19.11 (See color insert) A nondegenerate catenane. One of the rings (the moving ring) has two different recognition sites in it. Both sites can be turned "off" or "on" with different stimuli. When the green site is activated, the force and energy balance results in the first conformation, whereas when the red one is activated, the second conformation results. They can be named states 0 and 1 analogous to binary machine language.

19.2.3.3 Other Inorganic Molecular Machines

Many other molecular devices have been reported in the past four decades that bear a striking resemblance to macroscopic machinery. Chemical compounds behaving as bevel gears and propellers that were reported in the late 1960s and early 1970s are still being studied today [162–165]. A molecular propeller can be formed when two bulky rings such as the aryl rings [166] are connected to one central atom, often called the focal atom. Clockwise rotation of one such ring induces a counterclockwise rotation of the opposite ring about the bond connecting it to the central atom. It is possible to have a three-propeller system as well [167–169]. Triptycyl and amide ring systems have been shown to observe a coordinated gear-like rotation [170–174]. "Molecular Turnstiles" which are rotating plates inside a macrocycle, have been created [175,176]. Such rotations, however, were not controllable. A rotation of a molecular ring about a bond could be controlled by chemical stimuli, and this was shown by Kelly et al. [177] when they demonstrated a molecular brake. A propeller-like rotation of a 9-triptycyl ring system, which was used in gears, this time connected to a 2, 2′-bipyridine unit could be controlled by the addition and subsequent removal of a metal. Thus, free rotations along single bonds can be stopped and released at will.

Another type of molecular switch is the 1 "chiroptical molecular switch" [178]. Another large cyclic compound was found to be switchable between its two stable isomeric forms P and M′ (right and left handed) stimulated by light. Depending on the frequency of light bombarded on it the *cis* and the *trans* conformations of the compound 4-[9′(2′-meth-oxythioxanthylidene)]-7-methyl-1,2,3,4-tetrahydrophenanthrene can be interconverted. Allowing a slight variation to this switch, a striking molecular motor driven by light or heat or both was introduced by Koumura et al. [179]. As opposed to the rotation around a single bond in the ratchet described above, the rotation was achieved around a carbon–carbon double bond in a helical alkene. Ultraviolet light or the change in temperature could trigger a rotation involving four isomerization steps in the compound (3R,3′R)-(P,P)-*trans*-1,1′,2,2′,3,3′,4,4′-octahydro-3,3′-dimethyl-4,4′,-biphenanthrylidene. A second generation motor along with eight other motors from the same material is now operational [180]. This redesigned motor has distinct upper and lower portions and it

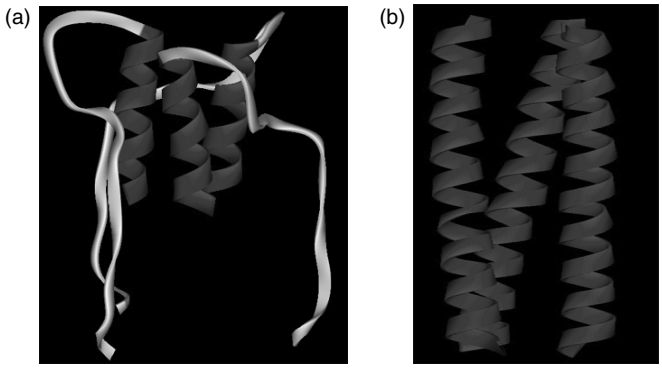

FIGURE 19.12 (See color insert) VPL motor at (a) neutral and (b) acidic pH. (a) Front view of the partially α-helical triple stranded coiled coil. VPL motor is in the closed conformation. (b) VPL Motor in the open conformation. The random coil regions (white) are converted into well-defined helices and an extension occurs at lower pH.

operates at a higher speed. This motor also provides a good example of how controlled motion at the molecular level can be used to produce a macroscopic change in a system that is visible to the naked eye. The light-driven motors when inside liquid crystal (LC) films can produce a color change by inducing a reorganization of mesogenic molecules [181].

19.2.4 Other Protein-Based Motors Under Development

In this section we present two protein-based motors that are at initial developmental stages and yet possess some very original and interesting characteristics.

19.2.4.1 Viral Protein Linear Motors

The idea of Viral Protein Linear (VPL) motors [182] stems from the fact that families of retroviruses like the influenza virus [183] and the HIV-1 [184] has a typical mechanism of infecting a human cell. When such a virus comes near the cell it is believed that due to the environment surrounding the cell it experiences a drop in pH of its surroundings. This is a kind of a signal to the virus that its future host is near. The drop in pH changes the energetics of the outer (envelope glycoprotein) protein of the viral membrane in such a way that there is a distinct conformational change in a part of it [185,186]. A triple stranded coiled coil domain of the membrane protein changes conformation from a loose random structure to a distinctive α-helical conformation [187]. It is proposed to isolate this domain from the virus and trigger the conformational change by variation of pH *in vitro*. Once this is realized, attachments can be added to the N or C (or both) terminals of the peptide and a reversible linear motion can be achieved. Figure 19.12 shows a triple stranded coiled coil structure at a pH of 7.0; the inverted hairpin-like coils shown in the front view in Figure 19.12(a) and top view in Figure 19.12(b) change conformation into extended helical coils as seen in Figure 19.12(b).

19.2.4.2 Synthetic Contractile Polymers

In a recent development, large plant proteins that can change conformation when stimulated by positively charged ions were separated from their natural environment and shown to exert forces in orthogonal directions [188,189]. Proteins from sieve elements of higher plants that are a part of the microfluidics system of the plant were chosen to build a new protein molecular machine element. These elements change conformations in the presence of Ca^{2+} ions and organize themselves inside the tubes so as to stop the fluid flow in case there is a rupture downstream. This is a natural defense mechanism seen in such plants. The change in conformation is akin to a balloon inflating and extending in its lateral as well as longitudinal directions. These elements, designated as "forisomes" adhered on to glass tubes were shown to reversibly swell in the presence of Ca^{2+} ions and shrink in their absence, hence performing a

pulling/pushing action in both directions. Artificially prepared protein bodies like the forisomes could be a useful molecular machine component in a future molecular assembly, producing forces of the order of micronewtons [188]. Unlike the ATP-dependant motors discussed previously, these machine elements are more robust because they can perform in the absence of their natural environment as well.

19.3 Nanorobotics Design and Control

19.3.1 Design of Nanorobotic Systems

The design of nanorobotic systems requires the use of information from a vast variety of sciences ranging from quantum molecular dynamics to kinematic analysis. In this chapter we assume that the components of a nanorobot are made of biological components, such as, proteins and DNAs. So far, there does not exist any particular guideline or a prescribed manner, which details the methodology of designing a bio-nanorobot. There are many complexities, which are associated with using biocomponents (such as protein folding and presence of aqueous medium), but the advantages of using these are also quite considerable. These biocomponents offer immense variety and functionality at a scale where creating a man-made material with such capabilities would be extremely difficult. These biocomponents have been perfected by nature through millions of years of evolution and hence these are very accurate and efficient. As noted in the review section on molecular machines, F_1-ATPase is known to work at efficiencies which are close to 100%. Such efficiencies, variety, and form are not existent in any other form of material found today. Also, the other significant advantages in using protein-based bio-nanocomponents is the development and refinement over the last 30 years of tools and techniques that enable researchers to mutate proteins in almost any way imaginable. These mutations can consist of anything from simple amino acid side-chain swapping, to amino acid insertions or deletions, incorporation of nonnatural amino acids, and even the combination of unrelated peptide domains into whole new structures. An excellent example of this approach is the engineering of the F_1-ATPase, which is able to rotate a nanopropeller in the presence of ATP. A computational algorithm [190] was used to determine the mutations necessary to engineer an allosteric zinc-binding site into the F_1-ATPase using site-directed mutagenesis. The mutant F_1-ATPase was then shown to rotate an actin filament in the presence of ATP with average torque of 34 pN nm. This rotation could be stopped with the addition of zinc, and restored with the addition of a chelator to remove the zinc from the allosteric binding site [191]. This type of approach can be used for the improvement of other protein-based nanocomponents.

Hence, these biocomponents seem to be a very logical choice for designing nanorobots. Some of the core applications of nanorobots are in the medical field and using biocomponents for these applications seems to be a good choice as they offer both efficiency and variety of functionality. This idea is clearly inspired by nature's construction of nanorobots, bacteria, and viruses which could be termed as *intelligent* organisms capable of movement, sensing, and organized control. Hence, our scope would be limited to the usage of these biocomponents in the construction of bio-nanorobotics. A roadmap is proposed which details the main steps towards the design and development of bio-nanorobots.

19.3.1.1 The Roadmap

The roadmap for the development of bio-nanorobotic systems for future applications (medical, space, and military) is shown in Figure 19.13. The roadmap progresses through the following main steps.

19.3.1.1.1 Step 1: Bio-Nanocomponents

Development of bio-nanocomponents from biological systems is the first step towards the design and development of an advanced bio-nanorobot, which could be used for future applications (see Figure 19.14). Since the planned systems and devices will be composed of these components, we must have a sound understanding of how these behave and how could they be controlled. From the simple elements such as structural links to more advanced concepts such as motors, each component must be carefully studied and possibly manipulated to understand the functional limits of each one of them. DNA and

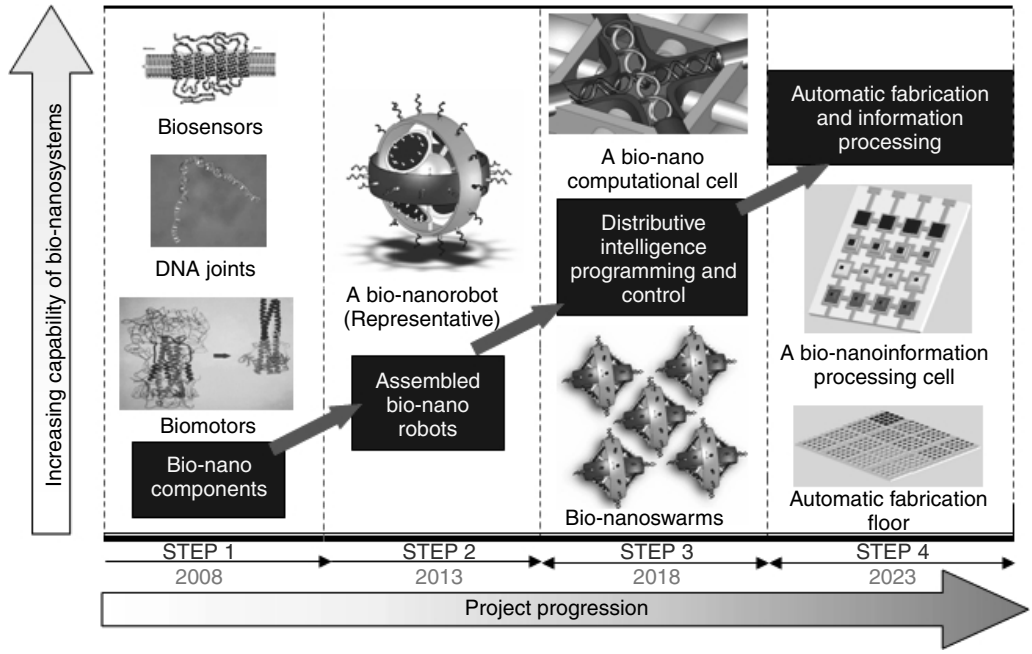

FIGURE 19.13 (See color insert) The roadmap, illustrating the system capability targeted as the project progresses.

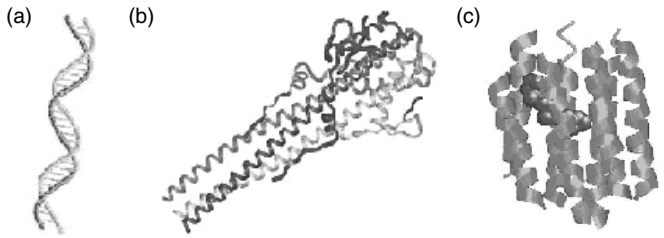

FIGURE 19.14 (Step 1) (See color insert) 5 years from now — understanding of basic biological components and controlling their functions as robotic components. Examples are: (a) DNA which may be used in a variety of ways such as a structural element and a power source; (b) hemagglutinin virus may be used as a motor; (c) bacteriorhodopsin could be used as a sensor or a power source.

carbon nanotubes are being fabricated into various shapes, enabling possibilities of constructing newer and complex devices. These nanostructures are potential candidates for integrating and housing the bio-nanocomponents within them. Proteins such as *rhodopsin* and *bacteriorhodopsin* are a few examples of such bio-nanocomponents. Both these proteins are naturally found in biological systems as light sensors. They can essentially be used as solar collectors to gather abundant energy from the sun. This energy could either be harvested (in terms of proton motive force) for later use or could be consumed immediately by other components, such as the ATP Synthase nanorotary motor. The initial work is intended to be on the biosensors, such as, heat shock factor. These sensors will form an integral part of the proposed bio-nanoassemblies, where these will be integrated within a nanostructure and will get activated, as programmed, for gathering the required information at the nano scale. Tools and techniques from *molecular modeling* and *protein engineering* will be used to design these modular components.

19.3.1.1.2 Step 2: Assembled Bio-Nanorobots

The next step involves the assembly of functionally stable bio-nanocomponents into complex assemblies. Some examples of such complex assemblies or bio-nanorobots are shown in Figure 19.15. Figure 19.15(a)

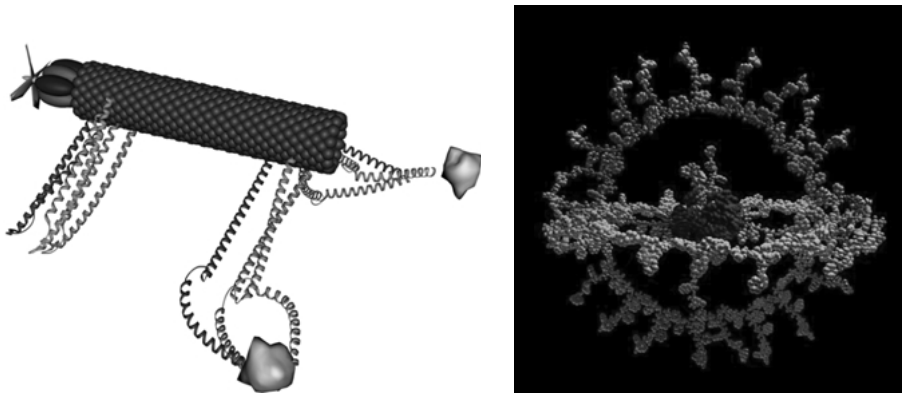

FIGURE 19.15 (Step 2) (See color insert) (a) The bio-nanocomponents will be used to fabricate complex biorobotic systems. A vision of a nano-organism: carbon nanotubes form the main body; peptide limbs can be used for locomotion and object manipulation and the biomolecular motor located at the head can propel the device in various environments. (b) Modular organization concept for the bio-nanorobots. Spatial arrangements of the various modules of the robots are shown. A single bio-nanorobot will have actuation, sensory, and information processing capabilities.

shows a bio-nanorobot with its "*feet*" made of helical peptides and its body of carbon nano tubes, while the power unit is a biomolecular motor. Figure 19.15(b) shows a conceptual representation of *modular organization* of a bio-nanorobot. The modular organization defines the hierarchy rules and spatial arrangements of various modules of the bio-nanorobots such as: the inner core (the brain/energy source for the robot); the actuation unit; the sensory unit; and the signaling and information processing unit. By the beginning of this phase a "*library of bio-nanocomponents*" will be developed, which will include various categories such as, actuation, energy source, sensory, signaling, etc. Thereon, one will be able to design and develop such bio-nanosystems that will have enhanced mobile characteristics, and will be able to transport themselves as well as other objects to desired locations at nano scale. Furthermore, some bio-nanorobots will have the capability of assembling various biocomponents and nanostructures from *in situ* resources to house fabrication sites and storage areas, while others will just manipulate existing structures by repairing damaged walls or making other renovations. There will also be robots that not only perform physical labor, but also sense the environment and react accordingly. There will be systems that will sense an oxygen deprivation and stimulate other components to generate oxygen, creating an environment with stable homoeostasis.

19.3.1.1.3 Step 3: Distributive Intelligence Programming and Control

With the individual bio-nanorobots in full function, they will now need to collaborate with one another to further develop systems and "colonies" of similar and diverse nanorobots. This step will lay the foundation to the concept of *bio-nanoswarms* (distributive bio-nanorobots) (see Figure 19.16[a]). Here work has to be performed towards control and programming of bio-nanoswarms. This will evolve concepts like distributive intelligence in the context of bio-nanorobots. Designing swarms of bio-nanorobots capable of carrying out complex tasks and capable of computing and collaborating amongst the group will be the focus. Therefore, the basic computational architectures need to be developed and rules need to be evolved for the bio-nanorobots to make intelligent decisions at the nano scale.

To establish an interface with the macroworld, the computers and electronic hardware have to be designed as well. Figure 19.17 shows the overall electronic communication architecture. From a location, humans should be able to control and monitor the behavior and action of these swarms. Also, the basic computational capabilities required for functioning of the swarms will be developed. A representative computational bio-nanocell, which will be deployed within a bio-nanorobot, is shown in Figure 19.16(b). This basic computational cell will initially be designed for data retrieval and storage at the nano scale. This capability will enable us to program (within certain degrees of freedom) the swarm behavior in the

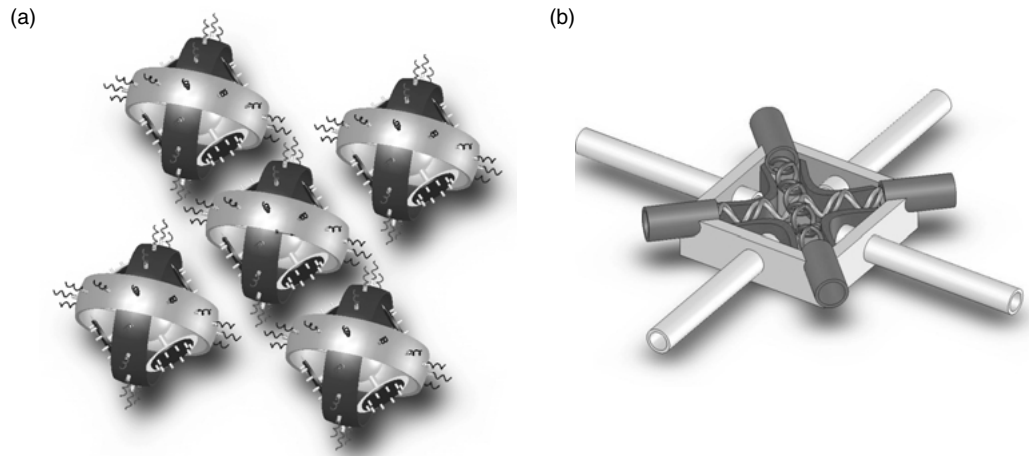

FIGURE 19.16 (Step 3) (See color insert) (a) Basic bio-nanorobot forming a small swarm of five robots. The spatial arrangement of the individual bio-nanorobot will define the arrangement of the swarm. Also, these swarms could be re-programmed to form bindings with various other types of robots. The number of robots making a swarm will be dependent of the resulting capability required by the mission. Also the capability of attaching new robots at run time and replacing the nonfunctional robots will be added. (b) A basic bio-nanocomputational cell. This will be based on one of the properties of the biomolecules, which is "reversibility."

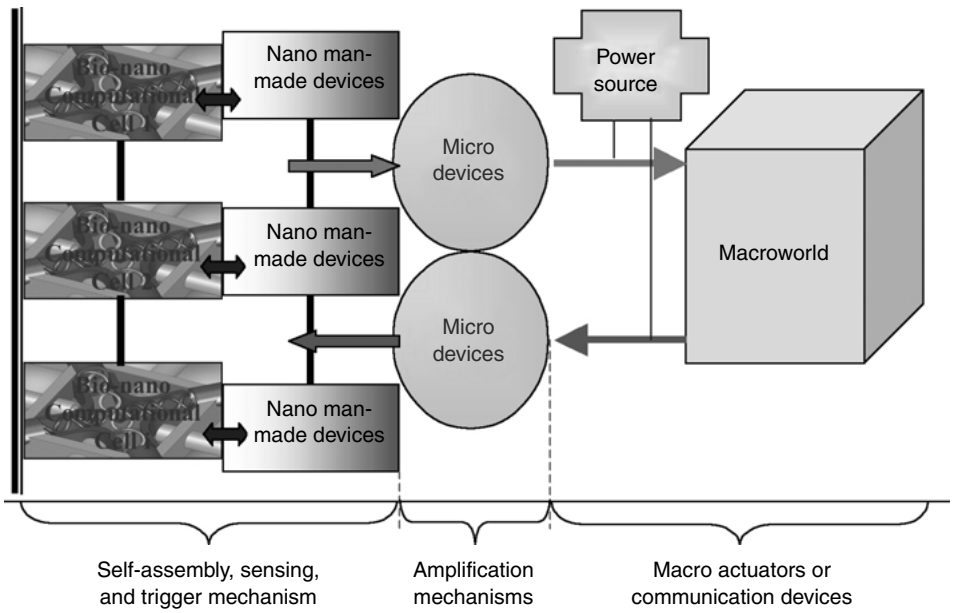

FIGURE 19.17 (See color insert) Feedback path from nano to macroworld route.

bio-nanorobots. We will further be able to get their sensory data (from nanoworld) back to the macroworld through these storage devices. This programming capability would form the core essence of a bio-nanorobotics system and hence enables them with immense power.

19.3.1.1.4 Step 4: Automatic Fabrication and Information Processing Machines

For carrying out complex missions, such as sensing, signaling, and storing, colonies of these bio-nanorobotic swarms need to be created. The next step in nanorobotic designing would see the emergence

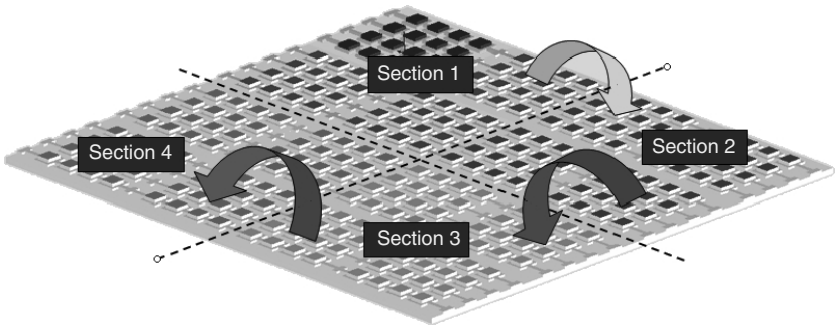

FIGURE 19.18 (Step 4): 20–30 years — an automatic fabrication floor layout. Different color represents different functions in automatic fabrication mechanisms. The arrows indicate the flow of components on the floor layout. *Section 1* → Basic stimuli storage — control expression; *Section 2* → Biomolecular component manufacturing (actuator/sensor); *Section 3* → Linking of bio-nanocomponents; *Section 4* → Fabrication of bio-nanorobots (assemblage of linked bio-nanocomponents).

of automatic fabrication methodologies (see Figure 19.18) of such bio-nanorobots *in vivo* and *in vitro*. Capability of information processing, which will involve learning and decision making abilities, will be a key consideration of this step. This would enable bioswarms to have capability of *self-evolving* based on the environment they will be subjected to. These swarms could be programmed to search for *alternate* energy sources and would have an ability to adapt as per that resource. Energy management, self-repairing, and evolving will be some of the characteristics of these swarms.

19.3.1.2 Design Philosophy and Architecture for the Bio-nanorobotic Systems

19.3.1.2.1 Modular Organization

Modular organization defines the fundamental rule and hierarchy for constructing a bio-nanorobotic system. Such construction is performed through *stable integration* of the individual "*bio-modules or components*," which constitute the bio-nanorobot. For example, if the entity ABCD, defines a bio-nanorobot having some *functional specificity* (as per the capability matrix defined in Table 19.1) then, A, B, C, and D are said to be the basic biomodules defining it. The basic construction will be based on the techniques of molecular modeling with emphasis on principles such as *Energy Minimization* on the hyper surfaces of the biomodules; *Hybrid Quantum-Mechanical and Molecular Mechanical* methods; *Empirical Force field* methods; and *Maximum Entropy Production* in least time.

Modular organization also enables the bio-nanorobots with capabilities such as, organizing into *swarms*, a feature, which is extremely desirable for various applications. Figure 19.19(a) and (b) shows the conceptual representation of modular organization. Figure 19.19(c) shows a more realistic scenario in which all the modules are defined in some particular spatial arrangements based on their functionality and structure. A particular module could consist of other group of modules, just like a fractal structure (defined as *fractal modularity*). The concept of *bio-nanocode* has been devised, which basically describes the unique functionality of a bio-nanocomponent in terms of alphabetic codes. Each bio-nanocode represents a particular module defining the structure of the bio-nanorobot. For instance, a code like E-M-S will describe a bio-nanorobot having capabilities of energy storage, mechanical actuation, and signaling at the nano scale. Such representations will help in general classifications and representative mathematics of bio-nanorobots and their swarms. Table 19.1 summarizes the proposed capabilities of the biomodules along with their targeted general applications. The bio-nanocode EIWR‖M‖S‖FG representing the bio-nanosystem shown in Figure 19.19(b) which could be decoded as shown in Figure 19.20. This depicts the "*Fractal modularity*" principle of the proposed concept.

19.3.1.2.2 The Universal Template — Bio-Nanostem System

The modular construction concept involves designing a universal template for bio-nanosystems, which could be "programmed and grown" into any possible bio-nanocoded system. This concept mimics the

TABLE 19.1 Defining the Capability Matrix for the Biomodules

Functionality	Bionanocode	Capabilities targeted	General applications
Energy storage and carrier	E	Ability to store energy from various sources such as, solar, chemical for future usage and for its own working	Required for the working of all the biochemical mechanisms of the proposed bio-nanorobotic systems
Mechanical	M	Ability to precisely move and orient other molecules or modules at nano scale. This includes ability to mechanically bind to various target objects, and carry them at desired location	Carry drugs and deliver it to the precise locations Move micro world objects with nanoprecision. For example, *Parallel platforms* for nanoorientation and displacements
Sensory	S	Sensing capabilities in various domains such as, chemical, mechanical, visual, auditory, electrical, and magnetic	Evaluation and discovery of target locations based on either chemical properties, temperature, or others characteristics
Signaling	G	Ability to amplify the sensory data and communicate with biosystems or with the microcontrollers. Capability to identify their locations through various trigger mechanisms such as fluorescence	Imaging for medical applications or for imaging changes in nanostructures
Information storage	F	Ability to store information collected by the sensory element Behave similar to a read–write mechanism in computer field	Store the sensory data for future signaling or usage Read the stored data to carry out programmed functions Backbone for the sensory bio-module Store nanoworld phenomenon currently not observed with ease
Swarm behavior	W	Exhibit binding capabilities with "similar" bio-nanorobots so as to perform distributive sensing, intelligence, and action (energy storage) functions	All the tasks to be performed by the bio-nanorobots will be planned and programmed keeping in mind the swarm behavior and capabilities
Bio-nanointelligence	I	Capability of making decisions and performing intelligent functions	Ability to make decision
Replication	R	Replicate themselves when required	Replicate at the target site Replication of a particular biomodule as per the demand of the situation

embryonic stem cells found in the human beings, that are a kind of primitive human cells which give rise to all other specialized tissues found in a human fetus, and ultimately to all the three trillion cells in an adult human body. Our bio-nanostem system will act in a similar way. This universal growth template will be constituted of some basic bio-nanocodes, which will define the bio-nanostem system. This stem system will be designed in a manner that could enable it to be programmed at run-time to any other required biomodule. Figure 19.21 shows one such variant of the bio-nanostem system, having the bio-nanocode: EIWR‖M‖S‖FG and having enhanced sensory abilities.

19.3.1.3 Computational and Experimental Tools for Studying bio-nanorobotic Systems

19.3.1.3.1 Computational Methods [192–194]

Molecular modeling techniques in sync with extensive experimentations will form the basis for studying bio-nanorobotic systems. Some of the molecular modeling techniques that can be used are described below.

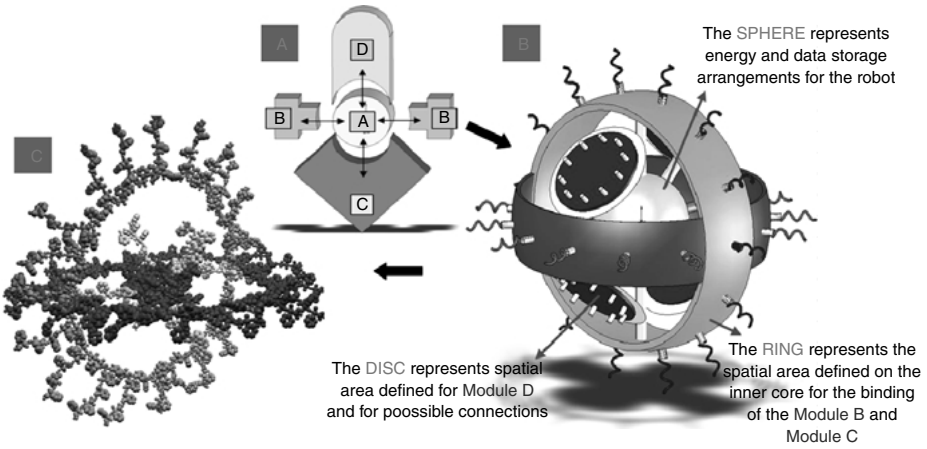

FIGURE 19.19 (See color insert)(a) A bio-nanorobotic Entity "ABCD," where A, B, C, and D are the various biomodules constituting the bio-nanorobot. In our case these biomodules will be set of stable configurations of various proteins and DNAs. (b) A bio-nanorobot (representative), as a result of the concept of modular organization. All the modules will be integrated in such a way so as to preserve the basic behavior (of self-assembly, self-replication, and self-organization) of the biocomponents at all the hierarchies. The number of modules employed is not limited to four or any number. It is a function of the various capabilities required for a particular mission. (c) A molecular representation of the figure (b). It shows the red core and green and blue sensory and actuation biomodules.

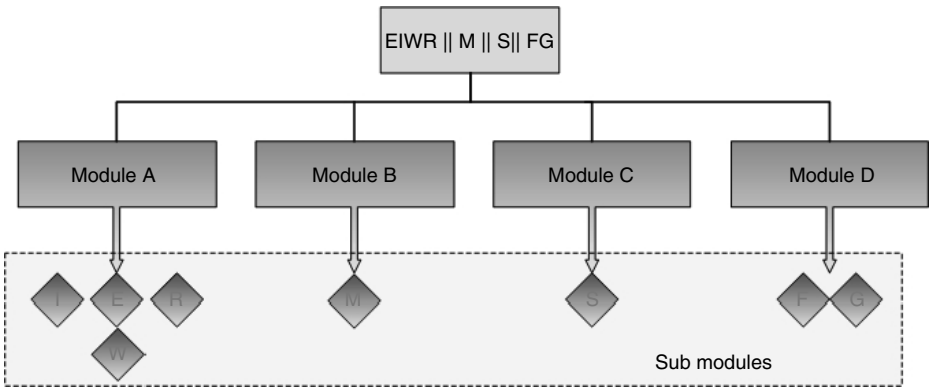

FIGURE 19.20 (See color insert) The bio-nanocode and the fractal modularity principle. The letter symbols have the values specified in Table 19.1. The "||" symbol integrates the various biomodules and collectively represents a higher order module or a bio-nanorobot.

19.3.1.3.1.1 Empirical Force Field Methods: (Molecular Mechanics) — In this method, the motion of the electrons is ignored and the energy of the system is calculated based on the position of the nucleus in a particular molecular configuration. There are several approximations which are used in this method with the very basic being the Born–Oppenheimer. The modeling of bio-nanocomponents or their assemblies could be done using one of the energy functions:

$$V(r^N) = \sum_{\text{bonds}} \frac{k_i}{2}(l_i - l_{i,0})^2 + \sum_{\text{angles}} \frac{k_i}{2}(\theta_i - \theta_{i,0})^2 + \sum_{\text{torsions}} \frac{v_n}{2}(1 + \cos(n\omega - \gamma))$$
$$+ \sum_{i=1}^{N} \sum_{j=i+1}^{N} \left(4\varepsilon_{ij} \left[\left(\frac{\sigma_{ij}}{r_{ij}} \right)^{12} - \left(\frac{\sigma_{ij}}{r_{ij}} \right)^{6} \right] + \frac{q_i q_j}{4\pi \varepsilon_o r_{ij}} \right)$$

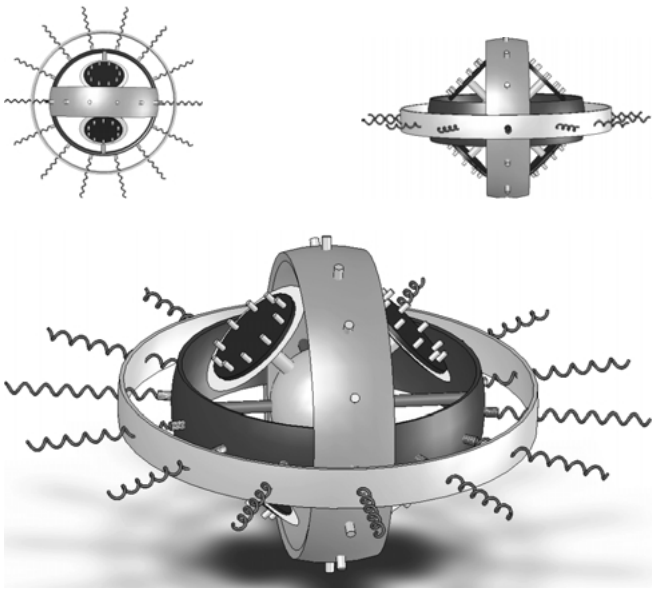

FIGURE 19.21 A variant of the initial bio-nanostem system (b), fabricated with enhanced bio-nanocode S, which defines it as a bio-nanorobot having enhanced sensory capabilities. The other features could be either suppressed or enhanced depending upon the requirement at hand. The main advantage of using bio-nanostem system is that we could at run-time decide which particular type of bio-nanorobots we require for a given situation. The suppression ability of the bio-nanostem systems is due to the property of "*Reversibility*" of the bio components found in living systems.

where $V(r^N)$ denotes the potential energy of N particles having position vector ($\mathbf{r}$). The terms of the previous equation are:

$\sum_{\text{bonds}} \frac{k_i}{2}(l_i - l_{i,0})^2$	Denotes the energy variations due to bond extension
$\sum_{\text{angles}} \frac{k_i}{2}(\theta_i - \theta_{i,0})^2$	Denotes the energy variations due to bond angle bending
$\sum_{\text{torsions}} \frac{v_n}{2}(1 + \cos(n\omega - \gamma))$	Denotes the energy variations due to bond torsion
$\sum_{i=1}^{N} \sum_{j=i+1}^{N} \left(4\varepsilon_{ij} \left[\left(\frac{\sigma_{ij}}{r_{ij}} \right)^{12} - \left(\frac{\sigma_{ij}}{r_{ij}} \right)^{6} \right] + \frac{q_i q_j}{4\pi \varepsilon_o r_{ij}} \right)$	Denotes the energy variation due to nonbonded terms, usually modeled using Coulomb's potential

19.3.1.3.1.2 Energy Minimization Methods — The potential energy depends upon the coordinates of the molecular configuration considered. In this method, points on the *hypersurface* (potential energy surface) are calculated for which the function has the minimum value. Such geometries, which correspond to the minimum energy, are the stable states of the molecular configuration considered. By this method we can also analyze the change in the configuration of the system from one minimum state to another. Methods such as the Newton–Raphson and Quasi-Newton are employed to calculate these minima. This method of finding minimum energy points in the molecule is used to prepare for other advanced calculations such

as molecular dynamics or Monte-Carlo simulations. It is further used to predict various properties of the system under study.

19.3.1.3.1.3 Molecular Dynamics Simulation Methods — To begin predicting the dynamic performance (i.e., energy and force calculation) of a biocomponent (say a peptide) molecular dynamics (MD) is performed. This method utilizes Newton's Law of motion through the successive configuration of the system to determine its dynamics. Another variant of molecular dynamics employed in the industry is the Monte-Carlo simulation, which utilizes stochastic approaches to generate the required configuration of a system. Simulations are performed based on the calculation of the free energy that is released during the transition from one configuration state to the other (e.g., using the MD software CHARMM, Chemistry at Harvard Molecular Mechanics, [195]). In MD, the feasibility of a particular conformation of a biomolecule is dictated by the energy constraints. Hence, a transition from one given state to another must be energetically favorable, unless there is an external impetus that helps the molecule overcome the energy barrier. When a macromolecule changes conformation, the interactions of its individual atoms with each other — as well as with the solvent — constitute a very complex force system. With one of the aspects of CHARMM, it is possible to model say, a peptide based on its amino acid sequence and allow a transition between two known states of the protein using targeted molecular dynamics (TMD) [196]. TMD is used for approximate modeling of processes spanning long time-scales and relatively large displacements.

19.3.1.3.1.4 Molecular Kinematic Simulations — They are also being used to study the geometric properties and conformational space of the biomolecules (peptides). The kinematic analysis is based on the development of direct and inverse kinematic models and their use towards the workspace analysis of the biomolecules. This computational study calculates all geometrically feasible conformations of the biomolecule, that is, all conformations that can be achieved without any atom interference. This analysis suggests the geometric paths that could be followed by a biomolecule during the transition from the initial to a final state, while molecular dynamics narrow downs the possibilities by identifying the only energetically feasible paths. The workspace analysis also characterizes the geometrically feasible workspace in terms of dexterity.

19.3.1.3.1.5 Modular Pattern Recognition and Clustering Function — The instantaneous value of the *property A* of a molecular system can be written as $A(p^n(t),\ r^n(t))$, where $p^n(t)$ and $r^n(t)$ represent the n momenta and positions of a molecular system at time t. This instantaneous value would vary with respect to the interactions between the particles. There are two parts to this function (termed as M function). One part (function A), evaluates and hence recognizes the equivalent modules (in term of properties) in the molecular system. The second part of the function (D) forms the cluster (like a bioisosteres, which are atom, molecules, or functional groups with similar physical and chemical properties) of various modular patterns according to the characteristic behaviors as identified by function A and also tracks their variations with rest to time.

$$M \equiv \{A(p^n(t), r^n(t), C^n[n]), D(A(p, r, C, t), f(x, y, \ldots), Bn(t))\}$$

where, *A is the first part* of the function; $p^n(t)$ and $r^n(t)$ represents the n momenta and positions of a molecular system at time t; and $C^n[n]$ is an n-dimensional matrix element for the individual components of the molecular system, which would store the categorized values of the modular patterns. D is the second part of the function, and it takes on function A recursively. It also maps these clusters based on a fitness function and stores the time-variant value in subfunction B. Figure 19.22, represents the conceptual version of the M-function.

This function is based on the hypothesis that in a complex molecular system, there are certain parts, which have similar properties and behavior as the system goes from one state to the other. By identifying these property patterns we can considerably reduce the simulation and computational

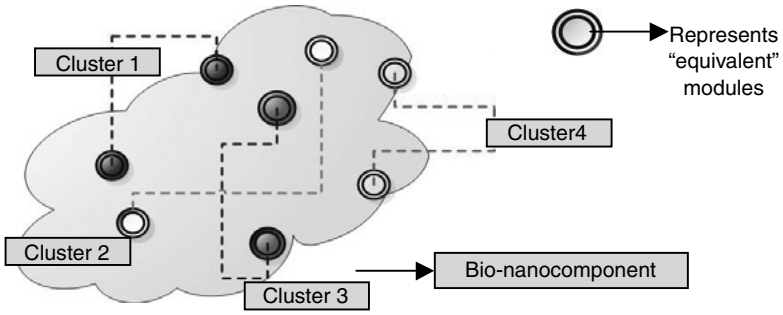

FIGURE 19.22 (See color insert) Representing the modular pattern recognition and clustering function (the *M*-function.)

time frames and can have better predictability of the system. Having established the design for the bio-nanocomponents, computational studies would focus on determining the overall design and architecture of the bio-nanoassemblies. One of the methods used in the industry is of molecular docking.

19.3.1.3.1.6 Molecular Docking and Scoring Functions — The molecular docking method is very important for the design of nanorobotic systems. This method is utilized to fit two molecules together in 3D space [197]. The method of molecular docking could be used to computationally design the bio-nanoassemblies. The algorithms like DOCK, genetic algorithms and distance geometry are being specifically explored. Many drug-design companies are using depth-first systematic conformational search algorithms for docking, and therefore, is a primary candidate for current research. The docking algorithm generates a large number of solutions. Therefore, we require scoring functions to refine the results so produced. Scoring functions in use today approximate the "*binding free energy*" of the molecules. The free energy of binding can be written as an additive equation of various components reflecting the various contributions to binding. A typical equation would be:

$$\Delta G_{\text{bind}} = \Delta G_{\text{solvent}} + \Delta G_{\text{cont}} + \Delta G_{\text{int}} + \Delta G_{\text{rot}} + \Delta G_{t/r} + \Delta G_{\text{vib}}$$

where, $\Delta G_{\text{solvent}}$ is the solvent effects contribution, ΔG_{conf} is due to conformational changes in the bio-molecule, ΔG_{int} due to specific molecular interactions, ΔG_{rot} due to restrictive internal rotation of the binding bio-molecules, $\Delta G_{t/r}$ is due to loss in the translational and rotational free energies due to binding, and ΔG_{vib} is due to vibrational mode variations. Once the overall architecture to bind the bio-nanocomponents is carried out through molecular docking, we will need to combine the components into real assemblies. The molecular component binding is the next step in the design scheme.

19.3.1.3.1.7 Connecting Bio-nanocomponents in a Binding Site — There are typically two approaches to design connectors for binding the bio-nanocomponents. One method searches the molecular database and selects a connector based on geometrical parameters. CAVEAT is a traditional routine, which employs this method. The other approach is to design a connector from scratch atom by atom. The geometrical parameters being known (as the configuration and the architecture was defined by molecular docking) these connectors are designed. A typical method employs designing molecular templates (which do not interfere with the basic geometry and design of the binding bio-nanocomponents) for defining a basic connector for binding the bio-nanocomponents. Feasibility of designing these connectors in real life is one challenge faced by molecular modelers. The minimum energy criterion is employed via the Metropolis Monte-Carlo simulation annealing method to select the basic structure of the final connector. Genetic algorithm approaches are also employed to generate such designs.

19.3.1.3.2 Experimental Methods

The step 1 in the roadmap requires that we have a library of biocomponents, which are characterized based on their potentials for using them for developing nanorobots. Various molecular techniques could be employed for assessing the usefulness of the biocomponents. For developing a nanorobot, we require the knowledge of the structure of the biocomponents used and the degree of conformational change that each element is capable of undergoing, and the environmental cues (e.g., T, pH) that induce these structural changes. Based on the computational methods detailed in the previous section, the following experimental techniques could be used to obtain this information.

19.3.1.3.2.1 Circular Dichroism Spectroscopy (CD) — CD spectroscopy can be utilized to gain insights into the secondary structure of each biomolecule such as peptides. In this technique, polarized far-UV light is used to probe the extent of secondary structure formation in solutions. This technique represents a proven method for estimating the structural composition of the nanorobotic elements during a change in environmental conditions. The effect of temperature on the structure of the nanorobotic elements can be evaluated by cooling the samples to $+1°C$ and then heating to $+85°C$, with a 5-min equilibration at each temperature interval. Intervals could be determined by first conducting CD scans with broad intervals, with subsequent narrowing as the location of the transition is identified. The effect of pH and ionic strength on the transitions could be monitored using separate, equilibrated preparations for each condition.

19.3.1.3.2.2 Förster Resonance Energy Transfer — Another method that can be used to rapidly assess the extent of conformational changes by the nanorobotic elements is FRET. In order to employ this method, the nanorobotic components have to be engineered to have cysteine residues at both ends. One end of the biocomponent then has to be labeled with a donor dye molecule (Alexa Fluor 488, Molecular Probes), and the other end labeled with an acceptor dye molecule (Alexa Fluor 594). The resulting FRET signal can be monitored with a laser (488 nm), whereby the signal changes would depend on the spatial separation of the ends of the bio component.

19.3.1.3.2.3 Nuclear Magnetic Resonance (NMR) — NMR is utilized to determine the exact 3D structure of the nanorobotic components. Although CD spectroscopy can be used to estimate the changes in the structural composition of the bio components, it does not provide the exact 3D configuration. This information can be obtained through the use NMR spectroscopy and the labeling of the biocomponent with NMR-active atoms. In addition to determining the endpoint structures of the components, NMR can also be used to follow the kinetics of the biomolecule conformational changes, in real time.

19.3.1.3.2.4 Laser-Based Optical Tweezers (LBOT) and Single-Molecule Fluorescence — LBOT and single-molecule fluorescence could be used to estimate the forces exerted by the nanorobotic elements, and the structural changes that occur during the genesis of these forces, after exposure to different stimuli. LBOT can provide force and displacement results with a resolution of sub-picoNewton and approximately one nanometer, respectively. Single-molecule fluorescence measurements, based on the previously described FRET method, can simultaneously provide information about the structural state of the molecule at each point of the force–displacement curve. To correlate force measurements with structural changes, combination of the LBOT method with FRET can be used [198]. The recent development of this technique has enabled the simultaneous assessment of nanoscale structural changes and their associated biomechanical forces.

19.3.1.4 Nanomanipulation — Virtual Reality-Based Design Techniques

For scanning and manipulating matter at the nanoscale, scanning tunneling microscopy (STM) [199], scanning electron microscopy (SEM), atomic force microscopy (AFM) [197] and scanned-probe microscope (SPM) [201] seem to be the common tools. Current work is mainly focused on using AFM nanoprobes for teleoperated physical interactions and manipulation at the nano scale. Precise manipulation could help scientists better understand the principles of nanorobots [202,203].

To achieve this it is essential to visualize the atom-to-atom interaction in real time and see the results in a fully immersive 3D environment. Also, to facilitate user input in nanorobotic systems it is essential to develop voice, gesture, and touch recognition features in addition to the conventional visualization and manipulation techniques. Virtual reality technology is applied here, which not only provides immersive visualization but also gives an added functionality of *navigation* and *interactive manipulation* of molecular graphical objects. VR technology comes to our aid by providing the experience of perception and interaction with the nanoworld through the use of sensors, effectors and interfaces in a simulated environment. These interfaces transform the signals occurring at nanoscale processes into signals at macrolevel and vice-versa. The requirement is that the communication with the nanoworld must be at high level and in real time, preferably in a natural, possibly intuitive "language." Considering the nanospecific problems related to task application, tools, and the interconnection technologies it leads to many flexible nanomanipulation concepts. They can range from pure master/slave teleoperation (through 3D visual/VR or haptic force feedback or both), over shared autonomy control (where, e.g., some degrees of freedom are teleoperated and other are operating autonomously) to fully autonomous operation.

In order to precisely control and manipulate biomolecules, we need tools that can interact with these objects at the nano scale in their native environments [204,205]. Existing bio-nanomanipulation techniques can be classified as noncontact manipulations including laser trapping [206,207] and electro-rotation [208], and contact manipulation referred to as mechanical stylus-, AFM- or STM-based nanomanipulation [209]. The rapid expansion of AFM studies in biology/biotechnology results from the fact that AFM techniques offer several unique advantages: *first*, they require little sample preparation, with native biomolecules usually being imaged directly; *second*, they can provide a 3D reconstruction of the sample surface in real space at ultra-high resolution; *third*, they are less destructive than other techniques (e.g., electron microscopy) commonly employed in biology; and *fourth*, they can operate in several environments, including air, liquid, and vacuum. Rather than drying the sample, one can image quite successfully with AFM in fluid. The operation of AFM in aqueous solution offers an unprecedented opportunity for imaging biological molecules and cells in their physiological environments and for studying biologically important dynamic processes in real time [210].

Currently, these bio-nanomanipulations are conducted manually, however, long training, disappointingly low success rates from poor reproducibility in manual operations, and contamination call for the elimination of direct human involvement. Furthermore, there are many sources of spatial uncertainty in AFM manipulation, for example, tip effects, thermal drift, slow creeping motion, and hysteresis. To improve the bio-nanomanipulation techniques, automatic manipulation must be addressed. Visual tracking of patterns from multiple views is a promising approach, which is currently investigated in autonomous embryo pronuclei DNA injection [210]. Interactive nanomanipulation can be improved by imaging 3D viewpoint in a virtual environment. Construction of a VR space in an off-line operation mode for trajectory planning combined with a real-time operation mode for vision tracking of environmental change ensures a complete "immersed" visual display. Figure 19.23 shows an example of 3D bio-micro/nanomanipulation system with a 3D VR model of the environment including the biocell, and carrying out the user viewpoint change in the virtual space [211].

19.3.1.4.1 Molecular Dynamics Simulations in Virtual Environment

Molecular dynamics simulations of complex molecular systems require enormous computational power and produces large amount of data in each step. The resulting data includes number of atoms per unit volume, atomic positions, velocity of each atom, force applied on each atom, and the energy contents. These results of MD simulations need to be visualized to give the user a more intuitive feel of what is happening. Haptic interaction used in conjunction with VR visualization helps the scientist to control/monitor the simulation progress and to get feedback from the simulation process as well [212]. Figure 19.24 shows the virtual reality visualization of molecular dynamics simulation. Figure 19.25 shows a VR representation of MD simulations in CAVE virtual environment.

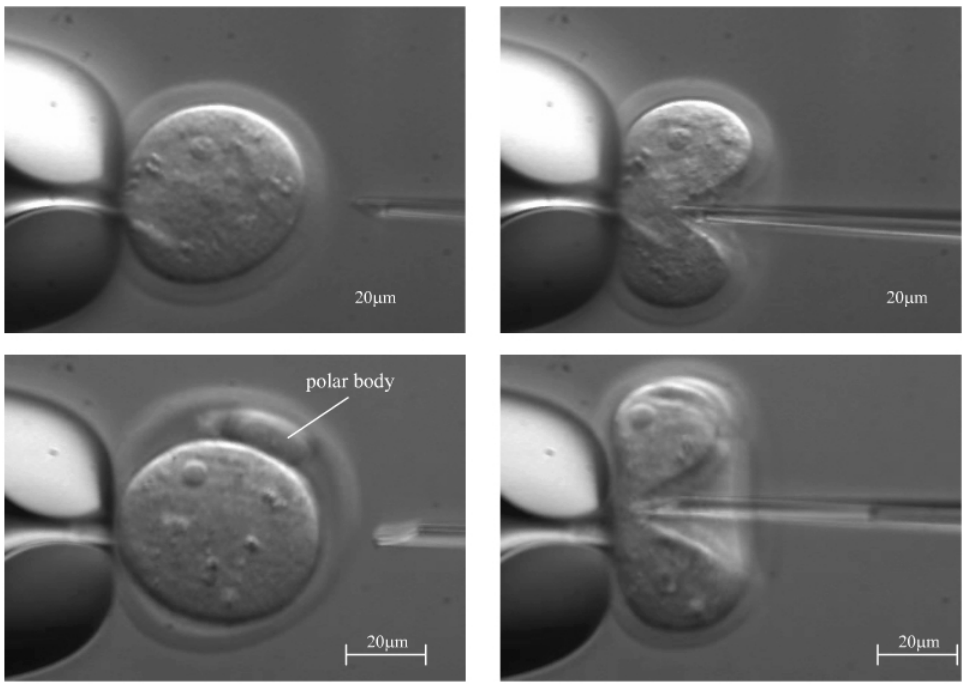

FIGURE 19.23 Haptic force measurement process on the Zona pellucida of mouse oocytes and embryos. (Courtesy of: Dr. Brad Nelson, Swiss Federal Institute of Technology (ETH), Zurich and ©2003 IEEE.)

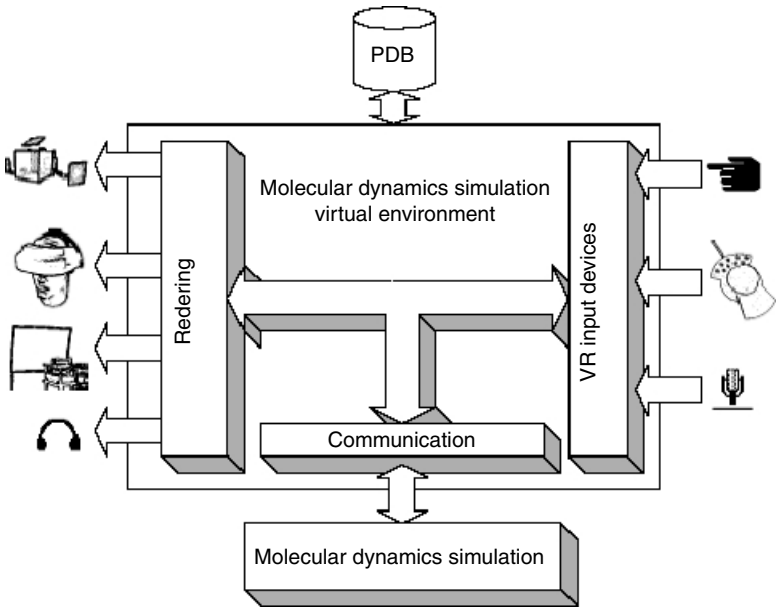

FIGURE 19.24 A block diagram showing virtual environment for molecular dynamics simulations (Reprinted from: Z. Ai and T. Frohlich, Molecular Dynamics Simulation in Virtual Environment, Computer Graphics Forum, Volume 17, September 1998. With permission from Eurographics Association.)

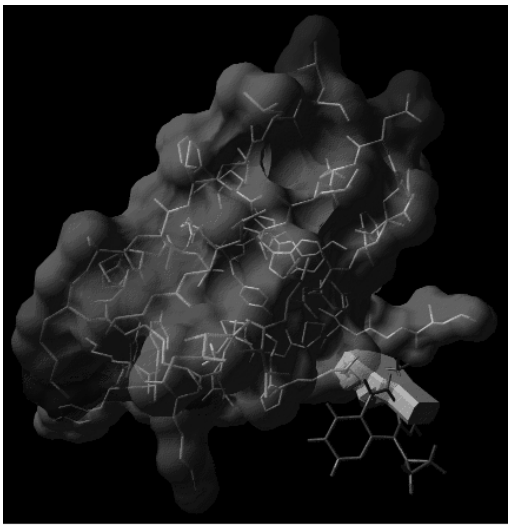

FIGURE 19.25 (See color insert) Molecular dynamics simulation visualized in the CAVE. (Courtesy of: Dr. Zhuming Ai, VRMedLab, University of Illinois at Chicago.)

19.3.2 Control of Nanorobotic Systems

The control of nanorobotic systems could be classified in two categories:

1. Internal control mechanisms
2. External control mechanisms

Another category could be a hybrid of internal and external control mechanisms.

19.3.2.1 Internal Control Mechanism — Active and Passive

This type of control depends upon the mechanism of biochemical sensing and selective binding of various biomolecules with various other elements. This is a traditional method, which has been in use since quite sometime for designing biomolecules. Using the properties of the various biomolecules and combining with the knowledge of the target molecule that is to be influenced, these mechanisms could be effective. But again, this is a passive control mechanism where at run time these biomolecules cannot change their behavior. Once programmed for a particular kind of molecular interaction, these molecules stick to that. Here lies the basic issue in controlling the nanorobots which are supposed to be intelligent and hence programmed and controlled so that they could be effective in the ever dynamic environment. The question of actively controlling the nanorobots using internal control mechanism is a difficult one. We require an "active" control mechanism for the designed nanorobots such that they can vary their behavior based on situations they are subjected to, similar to the way macrorobots perform. For achieving this internal control, the concept of molecular computers could be utilized. Leonard Adleman (from the University of Southern California) introduced DNA computers a decade ago to solve a mathematical problem by utilizing DNA molecules.

Professor Ehud Shapiro's lab (at Israel's Weizmann Institute) has devised a biomolecular computer which could be an excellent method for an internal 'active' control mechanism for nanorobots. They have recently been successful in programming the biomolecular computer to analyze the biological information, which could detect and treat cancer (prostate and a form of lung cancer) in their laboratory [213]. The molecular computer has an input and output module which acting together can diagnose a particular disease and in response produce a drug to cure that disease. It uses novel concept of software (made up of DNAs) and hardware (made up of enzymes) molecular elements. This molecular computer is in generalized form and can be used for any disease which produces a particular pattern of gene expression related to it [214].

19.3.2.2 External Control Mechanism

This type of control mechanism employs affecting the dynamics of the nanorobot in its work environment through the application of external potential fields. Researchers are actively looking at using MRI as an external control mechanism for guiding the nanoparticles. Professor Sylvain Martel's NanoRobotics Laboratory (at École Polytechnique de Montréal, Canada) is actively looking at using MRI system as a mean of propulsion for nanorobots. An MRI system is capable of generating variable magnetic field gradients, which can exert force on the nanorobot in the three dimensions and hence control its movement and orientation. Professor Martel's laboratory is exploring effect of such variable magnetic field on a ferromagnetic core that could probably be embedded into the nanorobots [215].

Other possibilities being explored are in the category of "hybrid" control mechanisms where the target is located and fixed by an external navigational system [216] but the behavior of the nanorobot is determined locally through an active internal control mechanism. The use of nanosensors and evolutionary agents to determine the nanorobots behavior is suggested by the mentioned reference.

19.4 Conclusions

Manipulating matter at molecular scale and influencing their behavior (dynamics and properties) is the biggest challenges for the nanorobotic systems. This field is still in very early stages of development and still a lot has to be figured out before any substantial outcome is produced.

The recent explosion of research in nanotechnology, combined with important discoveries in molecular biology have created a new interest in bio-nanorobotic systems. The preliminary goal in this field is to use various biological elements — whose function at the cellular level creates a motion, force, or a signal — as nanorobotic components that perform the same function in response to the same biological stimuli but in an artificial setting. In this way proteins and DNA could act as motors, mechanical joints, transmission elements, or sensors. If all these different components were assembled together they can form nanorobots and nanodevices with multiple degrees of freedom, with ability to apply forces and manipulate objects in the nanoscale world, transfer information from the nano- to the macroscale world and even travel in a nanoscale environment.

The ability to determine the structure, behavior, and properties of the nanocomponents is the first step which requires focused research thrust. Only when the preliminary results on these nanocomponents are achieved, steps towards actually building complex assemblies could be thought of. Still problems like protein (i.e., a basic bio-nanocomponent) folding and the precise mechanism behind the operation of the molecular motors like ATP Synthase have to be solved. The active control of nanorobots has to be further refined. Hybrid control mechanisms, wherein, a molecular computer and external (navigational) control system work in sync to produce the precise results seem very promising. Further, concepts like swarm behavior in context of nanorobotics is still to be worked out. As it would require colonies of such nanorobots for accomplishing a particular task, the concepts of cooperative behavior and distributed intelligence have to be evolved.

The future of bio-nanorobots (molecular robots) is bright. We are at the dawn of a new era in which many disciplines will merge including robotics, mechanical, chemical and biomedical engineering, chemistry, biology, physics, and mathematics so that fully functional systems will be developed. However, challenges towards such a goal abound. Developing a complete database of different biomolecular machine components and the ability to interface or assemble different machine components are some of the challenges to be faced in the near future.

References

[1] Drexler Eric K. 1992. *Nanosystems: Molecular Machinery, Manufacturing and Computation*: John Wiley & Sons.

[2] Kinosita K., Jr., Yasuda R., Noji H., Adachi K. 2000. A rotary molecular motor that can work at near 100% efficiency. *Philos. Trans.: Biol. Sci.* 355 (1396): 473–489.
[3] *The Nobel Foundation.* The Noble Prize in Chemistry 1997, April 10th, 2004, http://www.nobel.se/chemistry/educational/poster/1997/boyer-walker.html
[4] Antony Crofts, Lecture 10, ATP Synthase. University of Illinois at Urbana-Champaign, http://www.life.uiuc.edu/crofts/bioph354/lect10.html
[5] Lubert S. 1995. *Biochemistry, 4th edition*: W.H. Freeman and Company.
[6] Itoh H., Takahashi A., Adachi K., Noji H., Yasuda R., Yoshida M., and Kinosita K., Jr. 2004. Mechanically driven ATP synthesis by F_1-ATPase. *Nature* 427: 465–468.
[7] Howard J. 1997. Molecular motors: structural adaptations to cellular functions. *Nature* 389: 561–567.
[8] Vale R. 1996. Switches, latches, and amplifiers: common themes of G proteins and molecular motors. *J. Cell Biol.* 135: 291–302.
[9] Farrell C.M., Mackey A.T., Klumpp L.M., and Gilbert S.P. 2002. The role of ATP hydrolysis for kinesin processivity. *J. Biol. Chem.* 277: 17079–17087.
[10] Vale R.D. and Milligan R.A. 2000. The way things move: looking under the hood of molecular motor proteins. *Science* 288: 88–95.
[11] Block S.M., Goldstein L.S., and Schnapp B.J. 1990. Bead movement by single kinesin molecules studied with optical tweezers. *Nature* 348: 348–352.
[12] Howard J., Hudspeth A.J., and Vale R.D. 1989. Movement of microtubules by single kinesin molecules. *Nature* 342: 154–158.
[13] Finer J.T., Simmons R.M., and Spudich J.A. 1994. Single myosin molecule mechanics: piconewton forces and nanometre steps. *Nature* 368: 113–119.
[14] Hackney D.D. 1996. The kinetic cycles of myosin, kinesin, and dynein. *Annu. Rev. Physiol.* 58: 731–750.
[15] Block S.M. 1998. Kinesin, What Gives? *Cell* 93: 5–8.
[16] Kull F.J., Sablin E.P., Lau R., Fletterick R.J., and Vale R.D. 1996. Crystal structure of the kinesin motor domain reveals a structural similarity to myosin. *Nature* 380: 550–555.
[17] Sellers J.R. 2000. Myosins: a diverse superfamily. *Biochimica et Biophys. Acta (BBA) — Mol. Cell Res.* 1496: 3–22.
[18] Howard J. 1994. Molecular motors. Clamping down on myosin. *Nature* 368: 98–99.
[19] Huxley H.E. 1957. The double array of filaments in cross-striated muscle. *J. Biophys. Biochem. Cytol.* 3: 631–648.
[20] Huxley H.E. 1953. Electron microscope studies of the organisation of the filaments in striated muscle. *Biochimica et Biophys. Acta* 12: 387–394.
[21] Hanson J. and Huxley, H.E. 1953. Structural basis of the cross-striations in muscle. *Nature* 153: 530–532.
[22] Huxley H.E. 1969. The mechanism of muscular contraction. *Science* 164: 1356–1365
[23] Lymn R.W. and Taylor E.W. 1971. Mechanism of adenosine triphosphate hydrolysis by actomyosin. *Biochemistry* 10: 4617–4624.
[24] For videos of myosin and kinesin movement visit http://sciencemag.org/feature/data/1049155.shl
[25] Lowey S., Slayter H.S., Weeds A.G., and Baker H. 1969. Substructure of the myosin molecule. I. Subfragments of myosin by enzymic degradation. *J. Mol. Biol.* 42: 1–29.
[26] Weeds A.G. and Lowey S. 1971. Substructure of the myosin molecule. II. The light chains of myosin. *J. Mol. Biol.* 61: 701–725.
[27] Wagner P.D. and Giniger E. 1981. Hydrolysis of ATP and reversible binding to F-actin by myosin heavy chains free of all light chains. *Nature* 292: 560–562.
[28] Citi S. and Kendrick-Jones J. 1987. Regulation of non-muscle myosin structure and function. *Bioessays* 7: 155–159.
[29] Sellers J.R. 1991. Regulation of cytoplasmic and smooth muscle myosin. *Curr. Opin. Cell Biol.* 3: 98–104.

[30] Schroder R.R., Manstein D.J., Jahn W., Holden H., Rayment I. et al. 1993. Three-dimensional atomic model of F-actin decorated with Dictyostelium myosin S1. *Nature* 364: 171–174.
[31] Rayment I., Rypniewski W.R., Schmidt-Base K., Smith R., Tomchick D.R. et al. 1993. Three-dimensional structure of myosin subfragment-1: a molecular motor. *Science* 261: 50–58.
[32] Huxley A.F. 2000. Cross-bridge action: present views, prospects, and unknowns. *J. Biomech.* 33: 1189–1195.
[33] Huxley A.F. and Simmons R.M. 1971. Proposed mechanism of force generation in striated muscle. *Nature* 233: 533–538.
[34] Kabsch W., Mannherz H.G., Suck D., Pai E.F., and Holmes K.C. 1990. Atomic structure of the actin: DNase I complex. *Nature* 347: 37–44.
[35] Holmes K.C., Popp D., Gebhard W., and Kabsch W. 1990. Atomic model of the actin filament. *Nature* 347: 44–49.
[36] Spudich J.A. 1994. How molecular motors work. *Nature* 372: 515–518.
[37] Baker J.E., Brust-Mascher I., Ramachandran S., LaConte L.E., and Thomas D.D. 1998. A large and distinct rotation of the myosin light chain domain occurs upon muscle contraction. *Proc. Natl Acad. Sci. USA* 95: 2944–2949.
[38] Houdusse A., Kalabokis V.N., Himmel D., Szent-Gyorgyi A.G., and Cohen C. 1999. Atomic structure of scallop myosin subfragment S1 complexed with MgADP: a novel conformation of the myosin head. *Cell* 97: 459–470.
[39] Jontes J.D., Wilson-Kubalek E.M., and Milligan R.A. 1995. A 32 degree tail swing in brush border myosin I on ADP release. *Nature* 378: 751–753.
[40] Veigel C., Coluccio L.M., Jontes J.D., Sparrow J.C., Milligan R.A., and Molloy J.E. 1999. The motor protein myosin-I produces its working stroke in two steps. *Nature* 398: 530–533.
[41] Corrie J.E., Brandmeier B.D., Ferguson R.E., Trentham D.R., Kendrick-Jones J. et al. 1999. Dynamic measurement of myosin light-chain-domain tilt and twist in muscle contraction. *Nature* 400: 425–430.
[42] Irving M., St Claire Allen T., Sabido-David C., Craik J.S., Brandmeier B. et al. 1995. Tilting of the light-chain region of myosin during step length changes and active force generation in skeletal muscle. *Nature* 375: 688–691.
[43] Forkey J.N., Quinlan M.E., Shaw M.A., Corrie J.E., and Goldman Y.E. 2003. Three-dimensional structural dynamics of myosin V by single-molecule fluorescence polarization. *Nature* 422: 399–404.
[44] Vale R.D. and Milligan R.A. 2000. The way things move: looking under the hood of molecular motor proteins. *Science* 288: 88–95.
[45] Kitamura K., Tokunaga, M., Iwane, A.H., and Yanagida, T. 1999. A single myosin head moves along an actin filament with regular steps of ∼5.3 nm. *Nature* 397: 129–134.
[46] Howard J. 1996. The movement of kinesin along microtubules. *Annu. Rev. Physiol.* 58: 703–729.
[47] Howard J. and Hyman A.A. 2003. Dynamics and mechanics of the microtubule plus end. *Nature* 422: 753–758.
[48] Hirokawa N. 1998 Kinesin and dynein superfamily proteins and the mechanism of organelle transport. *Science* 279: 519–526.
[49] Vale R.D., Funatsu T., Pierce D.W., Romberg L., Harada Y., and Yanagida T. 1996. Direct observation of single kinesin molecules moving along microtubules. *Nature* 380: 451–453.
[50] Berliner E., Young E.C., Anderson K., Mahtani H.K., and Gelles J. 1995. Failure of a single-headed kinesin to track parallel to microtubule protofilaments. *Nature* 373: 718–721.
[51] Sablin E.P., Kull F.J., Cooke R., Vale R.D., and Fletterick R.J. 1996. Crystal structure of the motor domain of the kinesin-related motor ncd. *Nature* 380: 555–559.
[52] Sack S., Muller J., Marx A., Thormahlen M., Mandelkow E.M. et al. 1997. X-ray structure of motor and neck domains from rat brain kinesin. *Biochemistry* 36: 16155–16165.
[53] Schnitzer M.J. and Block S.M. 1997. Kinesin hydrolyses one ATP per 8-nm step. *Nature* 388: 386–390.

[54] Peskin C.S. and Oster G. 1995. Coordinated hydrolysis explains the mechanical behavior of kinesin. *Biophys. J.* 68: 202–211.
[55] Lohman T.M., Thorn K., and Vale R.D. 1998. Staying on track: common features of DNA helicases and microtubule motors. *Cell* 93: 9–12.
[56] Hackney D.D. 1995. Highly processive microtubule-stimulated ATP hydrolysis by dimeric kinesin head domains. *Nature* 377: 448–450.
[57] Hunt A.J., Gittes F., and Howard J. 1994. The force exerted by a single kinesin molecule against a viscous load. *Biophys. J.* 67: 766–781.
[58] Svoboda K. and Block S.M. 1994. Force and velocity measured for single kinesin molecules. *Cell* 77: 773–784.
[59] Gibbons I.R. and Rowe, A.J. 1965. Dynein: a protein with adenosine triphosphate activity from cilia. *Science* 149: 424–426.
[60] Schroer T.A., Steuer E.R., and Sheetz M.P. 1989. Cytoplasmic dynein is a minus end-directed motor for membranous organelles. *Cell* 56: 937–946.
[61] Schnapp B.J. and Reese T.S. 1989. Dynein is the motor for retrograde axonal transport of organelles. *Proc. Natl Acad. Sci. USA* 86: 1548–1552.
[62] Lye R.J., Porter M.E., Scholey J.M., and McIntosh J.R. 1987. Identification of a microtubule-based cytoplasmic motor in the nematode *C. elegans. Cell* 51: 309–318.
[63] Paschal B.M., Shpetner H.S., and Vallee R.B. 1987. MAP 1C is a microtubule-activated ATPase which translocates microtubules in vitro and has dynein-like properties. *J. Cell Biol.* 105: 1273–1282.
[64] Hirokawa N., Sato-Yoshitake R., Yoshida T., and Kawashima T. 1990. Brain dynein (MAP1C) localizes on both anterogradely and retrogradely transported membranous organelles *in vivo. J. Cell Biol.* 111: 1027–1037.
[65] Waterman-Storer C.M., Karki S.B., Kuznetsov S.A., Tabb J.S., Weiss D.G. et al. 1997. The interaction between cytoplasmic dynein and dynactin is required for fast axonal transport. *Proc. Natl Acad. Sci. USA* 94: 12180–12185.
[66] Lin S.X. and Collins C.A. 1992. Immunolocalization of cytoplasmic dynein to lysosomes in cultured cells. *J. Cell. Sci.* 101 (Pt 1): 125–137.
[67] Corthesy-Theulaz I., Pauloin A., and Rfeffer S.R. 1992. Cytoplasmic dynein participates in the centrosomal localization of the Golgi complex. *J. Cell Biol.* 118: 1333–1345.
[68] Aniento F., Emans N., Griffiths G., and Gruenberg J. 1993. Cytoplasmic dynein-dependent vesicular transport from early to late endosomes. *J. Cell Biol.* 123: 1373–1387.
[69] Fath K.R., Trimbur G.M., and Burgess D.R. 1994. Molecular motors are differentially distributed on Golgi membranes from polarized epithelial cells. *J. Cell Biol.* 126: 661–675.
[70] Blocker A., Severin F.F., Burkhardt J.K., Bingham J.B., Yu H. et al. 1997. Molecular requirements for bi-directional movement of phagosomes along microtubules. *J. Cell Biol.* 137: 113–129.
[71] King S.J., Bonilla M., Rodgers M.E., and Schroer T.A. 2002. Subunit organization in cytoplasmic dynein subcomplexes. *Protein Sci.* 11: 1239–1250.
[72] King S.M. 2000. The dynein microtubule motor. *Biochim. Biophys. Acta* 1496: 60–75.
[73] Burgess S., Walker, M.L., Sakakibara, H., Knight, P.J., and Oiwa, K. 2003. Dynein Structure and Power Stroke. *Nature* 421: 715–718.
[74] Koonce M.P. 1997. Identification of a microtubule-binding domain in a cytoplasmic dynein heavy chain. *J. Biol. Chem.* 272: 19714–19718.
[75] Gill S., Schroer T., Szilak I., Steuer E., Sheetz M., and Cleveland D. 1991. Dynactin, a conserved, ubiquitously expressed component of an activator of vesicle motility mediated by cytoplasmic dynein. *J. Cell Biol.* 115: 1639–1650.
[76] Straube A., Enard W., Berner A., Wedlich-Soldner R., Kahmann R., and Steinberg G. 2001. A split motor domain in a cytoplasmic dynein. *EMBO J.* 20: 5091–5100.
[77] Vale R.D. 2000. AAA Proteins: lords of the ring. *J. Cell Biol.* 150: 13F–20.

[78] Neuwald A.F., Aravind L., Spouge J.L., and Koonin E.V. 1999. AAA+: a class of chaperone-like ATPases associated with the assembly, operation, and disassembly of protein complexes. *Genom. Res.* 9: 27–43.
[79] Confalonieri F. and Duguet, M. 1995. A 200-amino acid ATPase module in search of a basic function. *BioEssays* 17: 639–650.
[80] King S.M. 2000. AAA domains and organization of the dynein motor unit. *J. Cell Sci.* 113 (Pt 14): 2521–2526.
[81] Asai D.J. and Koonce M.P. 2001. The dynein heavy chain: structure, mechanics and evolution. *Trends Cell Biol.* 11: 196–202
[82] Berry R.M. and Armitage J.P. 1999. The bacterial flagella motor. *Adv. Microb. Physiol.* 41: 291–337.
[83] Berg H.C. 2003. The rotary motor of bacterial flagella. *Ann. Rev. Biochem.* 72: 19–54.
[84] Blair D.F. 1995. How bacteria sense and swim. *Annu. Rev. Microbiol.* 49: 489–522.
[85] Berg H.C. and Anderson R.A. 1973. Bacteria swim by rotating their flagellar filaments. *Nature* 245: 380–382.
[86] Fahrner K.A., Ryu W.S., and Berg H.C. 2003. Biomechanics: bacterial flagellar switching under load. *Nature* 423: 938.
[87] Berg H.C. 2000. Motile behavior of bacteria. *Phys. Today* 53: 24–29.
[88] Scharf B.E., Fahrner K.A., Turner L., and Berg H.C. 1998. Control of direction of flagellar rotation in bacterial chemotaxis. *Proc. Natl Acad. Sci. USA* 95: 201–206.
[89] Macnab R.M. 1977. Bacterial flagella rotating in bundles: a study in helical geometry. *Proc. Natl Acad. Sci. USA* 74: 221–225.
[90] Elston T.C. and Oster G. 1997. Protein turbines. I: The bacterial flagellar motor. *Biophys. J.* 73: 703–721.
[91] Walz D. and Caplan S.R. 2000. An electrostatic mechanism closely reproducing observed behavior in the bacterial flagellar motor. *Biophys. J.* 78: 626–651.
[92] Schmitt R. 2003. Helix rotation model of the flagellar rotary motor. *Biophys. J.* 85: 843–852.
[93] Iino T., Komeda Y., Kutsukake K., Macnab R.M., Matsumura P. et al. 1988. New unified nomenclature for the flagellar genes of *Escherichia coli* and *Salmonella typhimurium. Microbiol. Rev.* 52: 533–535.
[94] Berg H.C. 1974. Dynamic properties of bacterial flagellar motors. *Nature* 249: 77–79.
[95] Ueno T., Oosawa K., and Aizawa S. 1992. M ring, S ring and proximal rod of the flagellar basal body of *Salmonella typhimurium* are composed of subunits of a single protein, FliF. *J. Mol. Biol.* 227: 672–677.
[96] Ueno T., Oosawa K., and Aizawa S. 1994. Domain structures of the MS ring component protein (FliF) of the flagellar basal body of *Salmonella typhimurium. J. Mol. Biol.* 236: 546–555.
[97] Driks A. and DeRosier D.J. 1990. Additional structures associated with bacterial flagellar basal body. *J. Mol. Biol.* 211: 669–672.
[98] Khan I.H., Reese T.S., and Khan S. 1992. The cytoplasmic component of the bacterial flagellar motor. *Proc. Natl Acad. Sci. USA* 89: 5956–5960.
[99] Francis N.R., Sosinsky G.E., Thomas D., and DeRosier D.J. 1994. Isolation, characterization and structure of bacterial flagellar motors containing the switch complex. *J. Mol. Biol.* 235: 1261–1270.
[100] Yorimitsu T. and Homma M. 2001. Na+-driven flagellar motor of *Vibrio. Biochimica et Biophy. Acta (BBA) — Bioenerg.* 1505: 82–93.
[101] Meister M., Lowe G., and Berg H.C. 1987. The proton flux through the bacterial flagellar motor. *Cell* 49: 643–650.
[102] Van Way S.M., Hosking E.R., Braun T.F., and Manson M.D. 2000. Mot protein assembly into the bacterial flagellum: a model based on mutational analysis of the motB gene. *J. Mol. Biol.* 297: 7–24.
[103] Blair D.F. and Berg H.C. 1988. Restoration of torque in defective flagellar motors. *Science* 242: 1678–1681.
[104] Fung D.C. and Berg H.C. 1995. Powering the flagellar motor of *Escherichia coli* with an external voltage source. *Nature* 375: 809–812.

[105] Berg H. and Turner L. 1993. Torque generated by the flagellar motor of *Escherichia coli. Biophys. J.* 65: 2201–2216.
[106] Chen X. and Berg H.C. 2000. Torque-speed relationship of the flagellar rotary motor of *Escherichia coli. Biophys. J.* 78: 1036–1041.
[107] Seeman N.C. 2003. DNA in a material world. *Nature* 421: 427–431.
[108] Dekker C.R. and M.A. 2001. Electronic properties of DNA. *Physics World*, pp. 29–33.
[109] Robinson B.H. and Seeman N.C. 1987. The design of a biochip: a self-assembling molecular-scale memory device. *Protein Eng.* 1: 295–300.
[110] Seeman N.C. and Belcher A.M. 2002. Emulating biology: building nanostructures from the bottom up. *PNAS* 99: 6451–6455.
[111] Smith S.B., Cui Y., and Bustamante C. 1996. Overstretching B-DNA: the elastic response of individual double-stranded and single-stranded DNA molecules. *Science* 271: 795–799.
[112] Simmel F.C. and Yurke B. 2001. Using DNA to construct and power a nanoactuator. *Phys. Rev. E Stat. Nonlin. Soft Matter Phys.* 63: 041913.
[113] Tinland B., Pluen A., Sturm J., and Weill G. 1997. Persistence length of single-stranded DNA. *Macromolecules* 30: 5763–5765.
[114] Seeman N.C. 1997. DNA Components for molecular architecture. *Accounts Chem. Res.* 30: 347–391.
[115] Niemeyer C.M. 1999. Progress in "engineering up" nanotechnology devices utilizing DNA as a construction material. *Appl. Phys. A: Materi. Sci. Process.* 68: 119–124.
[116] Chen J.H. and Seeman N.C. 1991. Synthesis from DNA of a molecule with the connectivity of a cube. *Nature* 350: 631–633.
[117] Zhang Y. and Seeman, N.C. 1994. Construction of a DNA-truncated octahedron. *J. Am. Chemical Soc.* 116: 1661–1669.
[118] Winfree E., Liu F., Wenzler L.A., and Seeman N.C. 1998. Design and self-assembly of two-dimensional DNA crystals. *Nature* 394: 539–544.
[119] Yan H., Zhang X., Shen Z., and Seeman N.C. 2002. A robust DNA mechanical device controlled by hybridization topology. *Nature* 415: 62–65.
[120] Mao C., Sun W., and Seeman N.C. 1997. Assembly of Borromean rings from DNA. *Nature* 386: 137–138.
[121] Mao C., LaBean T.H., Relf J.H., and Seeman N.C. 2000. Logical computation using algorithmic self-assembly of DNA triple-crossover molecules. *Nature* 407: 493–496.
[122] Simmel F.C. and Yurke, B., DNA-based Nanodevices. http://www2.nano.physik.uni-muenchen.de/publikationen/Preprints/index.html
[123] Coppin C.M., Pierce D.W., Hsu L., and Vale R.D. 1997. The load dependence of kinesin's mechanical cycle. *Proc. Natl Acad. Sci. USA* 94: 8539–8544.
[124] Seeman N.C. 1991. Construction of three-dimensional stick figures from branched DNA. *DNA Cell Biol.* 10: 475–486.
[125] Wang H., Du S.M., and Seeman N.C. 1993. Tight single-stranded DNA knots. *J. Biomol. Struct. Dyn.* 10: 853–863.
[126] Seeman N.C. 1998. Nucleic acid nanostructures and topology. *Angewandte Chemie International Edition* 37: 3220–3238.
[127] Mao C., Sun, W., and Seeman, N.C. 1999. Designed two-dimensional DNA Holliday junction arrays visualized by atomic force microscopy. *J. Am. Chemical Soc.* 121: 5437–5443.
[128] LaBean T.H., Yan, H., Kopatsch, J., Liu, F., Winfree, E., Reif, J.H., and Seeman, N.C. 2000. Construction, analysis, ligation, and self-assembly of DNA triple crossover complexes. *J. Am. Chemical Soc.* 122: 1848–1860.
[129] Fu T.J. and Seeman N.C. 1993. DNA double-crossover molecules. *Biochemistry* 32: 3211–3220.
[130] Zhang S., Fu T.J., and Seeman N.C. 1993. Symmetric immobile DNA branched junctions. *Biochemistry* 32: 8062–8067.

[131] Li X., Yang, X., Jing, Q., and Seeman, N.C. 1996. Antiparallel DNA double crossover molecules as components for nanoconstruction. *J. Am. Chemical Soc.* 118: 6131–6140.
[132] Mao C., Sun W., Shen Z., and Seeman N.C. 1999. A nanomechanical device based on the B-Z transition of DNA. *Nature* 397: 144–146.
[133] Rich A., Nordheim, A., and Wang A.H.-J. 1984. The chemistry and biology of left handed Z-DNA. *Ann. Rev. Biochem.* 53: 791–846.
[134] Pohl F.M. and Jovin T.M. 1972. Salt-induced co-operative conformational change of a synthetic DNA: equilibrium and kinetic studies with poly (dG-dC). *J. Mol. Biol.* 67: 375–396.
[135] Yurke B., Turberfield, A.J., Mills, A.P., Simmel, F.C., and Neumann, J.L. 2000. A DNA-fuelled molecular machine made of DNA. *Nature* 415: 62–65.
[136] Simmel F.C. and Yurke, B. 2002. A DNA-based molecular device switchable between three distinct mechanical states. *Appl. Phys. Lett.* 80: 883–885.
[137] Mitchell J.C. and Yurke, B. 2002. DNA Scissors. In *DNA Computing, Proceedings of the 7th International Meeting on DNA-Based Computers, DNA7*, S.N. Jonoska and Seeman N.(Eds.), Tampa, Florida: Springer Verlag, Heidelberg.
[138] Schill G. 1971. *Catenanes Rotaxanes and Knots.* New York: Academic Press.
[139] Ashton P.R., Ballardini, R., Balzani, V., Belohradsky, M., Gandolfi, M.T., Philp, D., Prodi, L., Raymo, F.M., Reddington, M.V., Spencer, N., Stoddart, J.F., Venturi, M., and Williams, D.J. 1996. Self-assembly, spectroscopic, and electrochemical properties of [n]rotaxanes. *J. Am. Chemical Soc.* 118: 4931–4951.
[140] Amabilino D.B., Asakawa, M., Ashton, P.R., Ballardini, R., Balzani, V., Belohradsky, M., Credi, A., Higuchi, M., Raymo, F.M., Shimizu, T., Stoddart, J.F., Venturi, M., and Yase, K. 1998. Aggregation of self-assembling branched [n]rotaxanes. *N. J. Chem.* 9: 959–972.
[141] Sauvage J.-P. and Dietrich-Buchecker C. 1999. *Molecular Catenanes, Rotaxanes and Knots.* Weinheim: Wiley-VCH.
[142] Harada A. 2001. Cyclodextrin-based molecular machines. *Accounts Chem. Res.* 34: 456–464.
[143] Anelli P.-L., Spencer, N., and Stoddart, J.F. 1991. A molecular shuttle. *J. Am. Chemical Soc.* 113: 5131–5133.
[144] Balzani V.V., Credi A., Raymo F.M., and Stoddart J.F. 2000. Artificial molecular machines. *Angew. Chem. Int. Ed. Engl.* 39: 3348–3391.
[145] Schalley C.A., Beizai, K., and Vogtle, F., 2001. On the way to rotaxane-based molecular motors: studies in molecular mobility and topological chirality. *Accounts Chem. Res.* 34: 465–476.
[146] Gatti F.G., Leon S., Wong J.K.Y., Bottari G., Altieri A. et al. 2003. Photoisomerization of a rotaxane hydrogen bonding template: Light-induced acceleration of a large amplitude rotational motion. *PNAS* 100: 10–14.
[147] Bermudez V.V., Capron N., Gase T., Gatti F.G., Kajzar F. et al. 2000. Influencing intramolecular motion with an alternating electric field. *Nature* 406: 608–611.
[148] Fyfe M.C.T. and Stoddart, J.F. 1997. Synthetic supramolecular chemistry. *Accounts Chem. Res.* 30: 393–401.
[149] Whitesides G.M., Mathias J.P., and Seto C.T. 1991. Molecular self-assembly and nanochemistry: a chemical strategy for the synthesis of nanostructures. *Science* 254: 1312–1319.
[150] Ashton P.R., Goodnow T.T., Kaifer A.W., Reddington M.V., Slawin A.M.Z., Spencer N., Stoddart J.F., Vicent C., and Williams D.J. 1989. A [2]catenane made to order. *Angewandte. Chemie. Int. Ed. England* 28: 1396–1399.
[151] Deleuze M.S. 2000. Can Benzylic Amide [2]Catenane Rings Rotate on Graphite? *J. Am. Chem. Soc.* 122: 1130–1143.
[152] Raymo F.M., Houk, K.N., and Stoddart, J.F. 1998. Origins of selectivity in molecular and supramolecular entities: solvent and electrostatic control of the translational isomerism in [2]catenanes. *J. Org. Chem.* 63: 6523–6528.
[153] Sauvage J.-P. 1998. Transition metal containing rotaxanes and catenanes in motion: toward molecular machines and motors. *Accounts Chem. Res.* 31: 611–619.

[154] Cambron J.-C. and Sauvage, J.-P. 1998. Functional rotaxanes: from controlled molecular motions to electron transfer between chemically nonconnected chromophores. *Chem.- A Euro. J.* 4: 1362–1366.

[155] Blnco M.J., Jimenez, M.C., Chambron J.-C., Heitz, V., Linke, M., and Sauvage, J.-P. 1999. Rotaxanes as new architectures for photoinduced electron transfer and molecular motions. *Chem. Soc. Rev.* 28: 293–305.

[156] Leigh D.A., Murphy, A., Smart, J.P., Deleuze, M.S., and Zerbetto, F. 1998. Controlling the frequency of macrocyclic ring rotation in benzylic amide [2]catenanes. *J. Am. Chem. Soc.* 120: 6458–6467.

[157] Fujita M. 1999. Self-assembly OF [2]catenanes containing metals in their backbones. *Accounts Chem. Res.* 32: 53–61.

[158] Collier C.P., Mattersteig G., Wong E.W., Luo Y., Beverly K. et al. 2000. A [2]catenane-based solid state electronically reconfigurable switch. *Science* 289: 1172–1175.

[159] Balzani V.V., Gomez-Lopez, M., and Stoddart, J.F. 1998. Molecular Machines. *Accounts Chem. Res.* 31: 405–414.

[160] Johnston M.R., Gunter, M.J., and Warrener, R.N. 1998. Templated formation of multi-porphyrin assemblies resembling a molecular universal joint. *Chem. Commun.* 28: 2739–2740.

[161] Amabilino D.B., Anelli P.-L., Ashton P.R., Brown G.R., Cordova E., Godinez L.A., Hayes W., Kaifer A.E., Philip D., Slawin A.M.Z., Spencer N., Stoddart J.F., Tolley M.S., and Williams D.J. 1995. Molecular meccano. 3. Constitutional and translational isomerism in [2]catenanes and [n]pseudorotaxanes. *J. Am. Chem. Soc.* 117: 11142–11170.

[162] Vacek J. and Michl J. 1997. A molecular "Tinkertoy" construction kit: computer simulation of molecular propellers. *N. J. Chem.* 21: 1259–1268.

[163] Michl J. and Magnera T.F. 2002. Supramolecular chemistry and self-assembly special feature: two-dimensional supramolecular chemistry with molecular Tinkertoys. *PNAS* 99: 4788–4792.

[164] Vacek J. and Michl J. 2001. Molecular dynamics of a grid-mounted molecular dipolar rotor in a rotating electric field. *PNAS* 98: 5481–5486.

[165] Gimzewski J.K., Joachim C., Schlittler R.R., Langlais V., Tang H., and Johannsen I. 1998. Rotation of a single molecule within a supramolecular bearing. *Science* 281: 531–533.

[166] Gust D. and Mislow, K. 1973. Analysis of isomerization in compounds displaying restricted rotation of aryl groups. *J. Am. Chem. Soc.* 95: 1535–1547.

[167] Finocchiaro P., Gust, D., and Mislow, K. 1974. Correlated rotation in complex triarylmethanes. I. 32-Isomer system and residual diastereoisomerism. *J. Am. Chem. Soc.* 96: 3198–3205.

[168] Finocchiaro P., Gust, D., and Mislow, K. 1974. Correlated rotation in complex triarylmethanes. II. 16- and 8-Isomer systems and residual diastereotopicity. *J. Am. Chem. Soc.* 96: 3205–3213.

[169] Mislow K. 1976. Stereochemical consequences of correlated rotation in molecular propellers. *Accounts Chem. Res.* 9: 26–33.

[170] Clayden J. and Pink, J.H. 1998. Concerted rotation in a tertiary aromatic amide: towards a simple molecular gear. *Angewandte. Chem. Int. Ed. Engl.* 37: 1937–1939.

[171] Hounshell W.D., Johnson, C.A., Guenzi, A., Cozzi,F., and Mislow, K. 1980. Stereochemical consequences of dynamic gearing in substituted bis (9-triptycyl) methanes and related molecules. *Proc. Natl Acad. Sci. USA* 77: 6961–6964.

[172] Cozzi F., Guenzi, A., Johnson, C.A., Mislow, K., Hounshell, W.D., and Blount, J.F. 1981. Stereoisomerism and correlated rotation in molecular gear systems. Residual diastereomers of bis(2,3-dimethyl-9-triptycyl)methane. *J. Am. Chem. Soc.* 103: 957–958.

[173] Kawada Y.I.H. 1981. Bis(4-chloro-1-triptycyl) ether. Separation of a pair of phase isomers of labeled bevel gears. *J. Am. Chem. Soc.* 103: 958–960.

[174] Johnson C.A., Guenzi, A., and Mislow, K. 1981. Restricted gearing and residual stereoisomerism in bis(1,4-dimethyl-9-triptycyl)methane. *J. Am. Chem. Soc.* 103: 6240–6242.

[175] Bedard TCMJS. 1995. Design and synthesis of a "molecular turnstile." *J. Am. Chem. Soc.* 117: 10662–10671.

[176] Ugi I., Marquarding, D., Klusacek, H., Gillespie, P., and Ramirez, F. 1971. Berry pseudorotation and turnstile rotation. *Accounts Chem. Res.* 4: 288–296.
[177] Kelly T.R., Bowyer M.C., Bhaskar K.V., Bebbington D., Garcia A., Lang F., Kim M.H., and Jette M.P. 1994. A molecular brake. *J. Am. Chem. Soc.* 116: 3657–3658.
[178] Feringa B.L., Jager W.F., De Lange B., and Meijer E.W. 1991. Chiroptical molecular switch. *J. Am. Chem. Soc.* 113: 5468–5470.
[179] Koumura N., Zijlstra R.W., van Delden R.A, Harada N., and Feringa B.L. 1999. Light-driven monodirectional molecular rotor. *Nature* 401: 152–155.
[180] Koumura N., Geertsema E.M., van Gelder M.B., Meetsma A., and Feringa B.L. 2002. Second generation light-driven molecular motors. Unidirectional rotation controlled by a single stereogenic center with near-perfect photoequilibria and acceleration of the speed of rotation by structural modification. *J. Am. Chem. Soc.* 124: 5037–5051.
[181] van Delden R.A., Koumura N., Harada N., and Feringa B.L.. 2002. Unidirectional rotary motion in a liquid crystalline environment: color tuning by a molecular motor. *Proc. Natl Acad. Sci. USA* 99: 4945–4949.
[182] Dubey A., Thornton A., Nikitczuk K.P., Mavroidis C., and Yarmush M.L. 2003. Viral Protein Linear (VPL) Nano-Actuators. *Proceedings of the 2003 3rd IEEE Conference on Nanotechnology, San Francisco, USA*.
[183] Wilson I.A., Skehel J.J., and Wiley D.C. 1981. Structure of the haemagglutinin membrane glycoprotein of influenza virus at 3 A resolution. *Nature* 289: 366–373.
[184] Chan D.C., Fass D., Berger J.M., and Kim P.S. 1997. Core structure of gp41 from the HIV envelope glycoprotein. *Cell* 89: 263–273.
[185] Bentz J. 2000. Minimal aggregate size and minimal fusion unit for the first fusion pore of influenza hemagglutinin-mediated membrane fusion. *Biophys. J.* 78: 227–245.
[186] Bentz J. 2000. Membrane fusion mediated by coiled coils: a hypothesis. *Biophys. J.* 78: 886–900
[187] Carr C.M. and Kim P.S. 1993. A spring-loaded mechanism for the conformational change of influenza hemagglutinin. *Cell* 73: 823–832.
[188] Knoblauch M., Noll G.A., Muller T., Prufer D., Schneider-Huther I. et al. 2003. ATP-independent contractile proteins from plants. *Nat. Mater.* 2: 600–603.
[189] Mavroidis C. and Dubey A. 2003. Biomimetics: From pulses to motors. *Nat. Mater.* 2: 573–574.
[190] Hellinga H.W. and Richards F.M. 1991. Construction of new ligand binding sites in proteins of known structure. I. Computer-aided modeling of sites with pre-defined geometry. *J. Mol. Biol.* 222: 763–785.
[191] Liu H., Schmidt J.J., Bachand G.D., Rizk S.S., Looger L.L. et al. 2002. Control of a biomolecular motor-powered nanodevice with an engineered chemical switch. *Nat. Mater.* 1: 173–177.
[192] Leach Andrew R. 2001: Molecular Modelling, Second Edition. *Prentice Hall.*
[193] Hinchliffe A. 2002. Modelling Molecular Structures, Second Edition. *Wiley & Sons.*
[194] Vinter J.G. and Gardner Mark. 1994: Molecular Modelling and Drug Design. *CRC Press.*
[195] Brooks R., Bruccoleri R.E., Olafson B.D, States D.J, Swaminathan S. et al. 1983. CHARMM: a program for macromolecular energy, minimization, and dynamics calculations. *J. Comput. Chem.* 4: 187–217.
[196] Schlitter J., Engels M., and Kruger P. 1994. Targeted molecular dynamics: a new approach for searching pathways of conformational transitions. *J. Mol. Graph.* 12: 84–89.
[197] Morris G.M. *Molecular Docking Web*, http://www.scripps.edu/pub/olson-web/people/gmm
[198] Lang M.J., Fordyce P.M., and Block S.M. 2003. Combined optical trapping and single-molecule fluorescence. *J. Biol.* 2: 6.
[199] Binnig G., Rohrer H., Gerber C., and Weibel E. 1986. Surface studies by scanning tunnelling microscopy, *Phys. Rev. Lett.*, 56: 930–933.
[200] Binnig G. 1982. Atomic force microscope, *Phys. Rev. Lett.*, 49: 57–61.
[201] Wickramasinghe H.K. 1989. Scanned-probe microscopes, *Sci. Am.*, 261: 89–105.

[202] Funatsu T., Harada Y., Higuchi H. et al. 1997. Imaging and nano-manipulation of single biomolecules, *Biophys. Chem.*, 68: 63–77.
[203] Svoboda K., Schmidt C., Schnapp B., and Block S. 1993. Direct observation of kinesin stepping by optical trapping interferometry, *Nature* 365: 721–727.
[204] Castelino K. Biological Object Nanomanipulation, *Review Report, University of California, Berkeley.*
[205] Fukuda T., Arai F., and Dong L. 2002. Nano Robotic World — From Micro to Nano, *Int'l Workshop on Nano- \Micro-Robotics in Thailand.*
[206] Ashkin A. 1970. Acceleration and trapping of particles by radiation pressure, *Phys. Rev. Lett.*, 24 (4): 156–156.
[207] Bruican T.N., Smyth M.J., Crissman H.A., Salzman G.C., Stewart C.C., and Martin J.C. 1987. Automated single-cell manipulation and sorting by light trapping, *Appl. Opt.*, 26 (24): 5311–5316.
[208] Nishioka M., Katsura S., Hirano K., and Mizuno A. 1997. Evaluation of cell characteristics by stepwise orientational rotation using optoelectrostatic micromanipulation, *IEEE Trans. Ind. Appl.*, 33 (5): 1381–1388.
[209] Riquicha A.A.G. et al. 2001. Manipulation of Nanoscale Components with the AFM: Principles and Applications, *IEEE Int. Conf. Nanotechnol.*, Maui, HI, October 28–30, 2001.
[210] Sun Y., Wan K.T., Roberts K.P., Bischof J.C., and Nelson B.J. 2003. Mechanical property characterization of the mouse zona pellucida, *IEEE Trans. NanoBioSci.*, 2 (4).
[211] Arai F. and Fukuda T. 1998. 3D Bio Micromanipulation , *International Workshop on Microfactoryies IWMF'98*, December 7–9, pp.143–148.
[212] Disz M., Papka M., Pellegrino Stevens R., and Taylor V. 1995. Virtual reality visualization of parallel molecular dynamics simulation, in Proc. 1995 Simulation Multi-conference Symposium, (Phoenix, Arizona), pp. 483 -487, *Society for Computer Simulation* (April 1995).
[213] Professor Shapiro: *Laboratory for Biomolecular Computers*: http://www.weizmann.ac.il/mathusers/lbn/index.html
[214] Benenson Y., Gil B., Ben-Dor U., Adar R., and Shapiro E. 2004. An autonomous molecular computer for logical control of gene expression. *Nature*, 429 (6990): 423–429.
[215] Mathieu J.-B., Martel S., Yahia L'H., Soulez G., and Beaudoin G. 2003. MRI Systems as a Mean of Propulsion for a Microdevice in Blood Vessels. *EMBC 2003.*
[216] Cavalcanti A., Freitas Robert A. Jr., and Kretly Luiz C. Nanorobotics control design: a practical approach tutorial. *ASME 28th Biennial Mechanisms and Robotics Conference*, Salt Lake City Utah, USA, September 2004.